**Centro de Investigación y de Estudios Avanzados
del Instituto Politécnico Nacional**

UNIDAD ZACATENCO
DEPARTAMENTO DE FÍSICA

**"MECÁNICA CUÁNTICA ESTOCÁSTICA EN
ESPACIOS CURVOS: APLICACIÓN A LOS
AGUJEROS NEGROS DE SCHWARZSCHILD"**

Tesis que presenta

Juan Sebastian Jerez Rodriguez

para obtener el Grado de

Maestro en Ciencias

en la Especialidad de

Física

Director de tesis:　**Dr. Tonatiuh Matos Chassin**

Ciudad de México

Enero, 2025

CENTRO DE INVESTIGACION Y DE ESTUDIOS AVANZADOS DEL INSTITUTO POLITECNICO NACIONAL

UNIT ZACATENCO
PHYSICS DEPARTMENT

ꞌꞌSTOCHASTIC QUANTUM MECHANICS IN CURVED SPACES: APPLICATION TO SCHWARZSCHILD BLACK HOLESꞌꞌ

Thesis submitted by

Juan Sebastian Jerez Rodriguez

In order to obtain the

Master of Science

degree, speciality in

Physics

Supervisor: **Dr. Tonatiuh Matos Chassin**

Mexico City   January, 2025

**Centro de Investigación y de Estudios
Avanzados del Instituto Politécnico Nacional
Unidad Zacatenco**

STOCHASTIC QUANTUM MECHANICS IN CURVED SPACES:

APPLICATION TO SCHWARZSCHILD BLACK HOLES

by

JUAN SEBASTIÁN JEREZ RODRÍGUEZ

ADVISOR: DR. TONATIUH MATOS CHASSIN

A thesis submitted to the

Department Physics at Cinvestav

in conformity with the requirements for

the degree of Master of Science in Physics

Dedication

 Dedicating something is not easy. I have seriously thought about who this writing is dedicated to, because at the end of the day, it is a scientific work and, if we are honest, beyond academia and research, no one else is going to read it. So, while I want those who read this to be interested in the subject, I want even more for those I appreciate and love (and who possibly cannot understand everything I say here) to feel fully proud that this thesis is for them (and by them). To the Jerez family—my aunts, uncle, cousins, and, above all, my grandparents—who have dedicated their lives so that my existence is full and happy. To the Rodríguez family (and especially to my grandmother, who is a being of light!), who brought into this world the most important person in my life, my mother. To Fernanda, who walks by my side every day, sees me grow, supports me, and loves me. To my mother, who is the fundamental pillar of what I am today; without her, I would be nothing. To my friends Carlos, Luz Angela, Valentina, Edwin, Erick, Noe, Oscar, Johan Chavez, Johan Caicedo, and to each one of those who accompany me and walk through my life: a thousand and one thanks for being and continuing to be. This is for you.

Without further ado, enjoy this text,

Juan.

Abstract

In this work, we study the possibility of applying Stochastic Quantum Mechanics to curved spacetimes, focusing on the Schwarzschild black hole. After reviewing general aspects of the metric and its $3 + 1$ decomposition, as well as the main concepts of stochastic quantum mechanics, we extend the quantum stochastic equations to include a curved spacetime by means of a covariant treatment. Next, we solve the Klein-Gordon equation for scalar perturbations, and analyze the resulting stochastic trajectories by varying parameters such as the angular momentum and the frequency of the particle. As a general conclusion, we find that the trajectories are influenced by the gravitational fluctuations of spacetime and that, depending on the varied fundamental parameters, different types of stochastic trajectories will be obtained.

Acknowledgements

Contents

Contents

Chapter 1

Introduction

Quantum mechanics and the theory of general relativity are fundamental pillars of current scientific knowledge. Since their inception, the behavior of particles in the presence of gravitational fields has been a topic of interest. For decades, physicists have failed to reach a consensus on a quantum theory of gravitation. Recently, Jonathan Oppenheim introduced an alternative approach to quantum field theory coupled to classical spacetime. This theory exhibits an essential stochastic nature which is studied through a master equation for the density matrix ρ, without the need for a "quantized" metric [1].

The basis of the present work is that, as a hypothesis, classical spacetime (considered as a smooth and differentiable manifold allowing geodesic trajectories between points) exhibits stochastic behavior. Escobar, Matos, and Aquino, by considering this stochasticity, infer that spacetime is no longer locally flat and obstructs such deterministic paths for sufficiently small particles, resulting in particles now following stochastic trajectories due to spacetime fluctuations (see [2]). They also demonstrate with this hypothesis that particles follow trajectories satisfying the Klein-Gordon

equation (in its Newtonian limit, the Schrödinger equation); all of the above using an approach where small test particles travel around geodesics with a stochastic term added to the trajectory. Their main conclusion is that the Schrödinger equation is a consequence of the stochastic structure of spacetime. The source of stochasticity in this framework is gravitational radiation (gravitational background waves, GWB), which originates from events such as black hole collisions, inflation, cosmic transitions, or the Big Bang, and permeates all of spacetime. This hypothesis is motivated by recent observations that reaffirm its existence (see [3, 4, 5, 6]).

The study of black holes has become fundamental since they represent extreme solutions to Einstein's field equations. The Schwarzschild metric, discovered by Karl Schwarzschild in 1916, was the first exact solution describing a static, chargeless black hole. Since then, numerous significant contributions have been made in this field. For example, Subrahmanyan Chandrasekhar predicted gravitational collapse (although very few believed him initially), Oppenheimer and Snyder demonstrated the collapse of a spherical star according to Einstein's theory, leading to the formation of a black hole, Roy Kerr discovered a solution to Einstein's equations that includes rotation, and Roger Penrose published his famous singularity theorem (Nobel Prize in Physics in 2020). The motivation to study black holes extends far beyond theoretical contributions. In recent years, Reinhard Genzel and Andrea Ghez, recipients of the 2020 Nobel Prize in Physics, discovered a supermassive object at the center of the Milky Way, concluding that it could only be explained by a black hole [7, 8, 9]. Additionally, multiple images captured recently, such as the one taken by the Event Horizon Telescope of the supermassive black hole M87* in the galaxy M87 in 2019,

and the confirmation of the Sgr A* black hole at the center of the Milky Way in 2022, provide experimental verification of these intriguing objects that we do not fully understand. Therefore, in this work, stochastic quantum mechanics is explored in the context of curved spacetime, with a particular focus on the Schwarzschild metric. The main objective is to investigate how stochastic quantum trajectories are affected by the presence of an intense gravitational field, such as that of the Schwarzschild black hole. To achieve this, the writing is divided into the following chapters:

In chapter 2, we define the Schwarzschild black hole-type solution in a rather general way, prove the geodesic equation, and analyze the decomposition of spacetime into its $3+1$ form.

In Chapter 3, we are guided by the work of L. de la Peña and A. M. Cetto and Nelson [10, 11] to provide a broad overview of the basic concepts of stochastic quantum mechanics.

Covariantization of stochastic quantum equations is discussed in Chapter 4, guided mainly by the results obtained by Escobar, Matos, and Aquino [2].

In Chapter 5, we study the solution of the Klein-Gordon equation for both massless and massive scalar fields in Schwarzschild spacetime and its respective application in stochastic quantum mechanics for curved spacetimes. We observe the stochastic trajectories of highly energetic photons, varying specific parameters such as the angular momentum l, the radial initial condition $r(0)$, and the particle frequency ω_0.

The last chapter is left for a summary and recapitulation of the most relevant conclusions.

Chapter 2

The Schwarzschild Black Hole and $3+1$ Split of Spacetime

General relativity is one of the most profound theories of modern physics, describing gravitational interaction as the curvature of space-time caused by matter and energy. At the core of this theory are Einstein's equations, which relate the geometry of space-time to its energy content, and are the basis for countless advances in theoretical physics.

One of the most relevant solutions to these equations is the Schwarzschild metric, which describes the empty spacetime around a static, uncharged, spherical object. When extended to radii smaller than the event horizon, this solution defines what we call a Schwarzschild black hole. A Schwarzschild black hole is an astrophysical object characterized by a spherical event horizon and a central singularity, where the curvature of spacetime becomes infinite. These black holes serve as ideal models for exploring the behavior of particles and fields in an extreme gravitational field. In this context, the motion of particles in this geometry is described by the geodesic

equation, which determines the natural trajectories in curved spacetime, both outside and inside the event horizon.

In order to analyze dynamical systems in general relativity, it is essential to reformulate the theory in such a way that it allows studying the temporal evolution of gravitational configurations. Here, the 3+1 decomposition of space-time comes into play, a formalism that separates spatial and temporal dimensions, facilitating the analysis of gravitational systems by means of restriction and evolution equations. This method is particularly relevant when one wants to connect the geometry of space-time with specific physical phenomena, as in the case of this thesis, the equations that describe quantum particles with a stochastic background.

In this chapter, we will first explore the geometric properties of the Schwarzschild solution, followed by an analysis of particle motion through the geodesic equation. Then, we will introduce the 3+1 decomposition, highlighting its usefulness in studying gravitational dynamics. This conceptual framework will be essential for future developments in this thesis.

2.1 Schwarzschild Black Holes

The Schwarzschild metric describes an empty spacetime that is spherically symmetric, i.e., it has no matter or energy present, and its geometry is the same in all directions around the central object. In spherical coordinates (t, r, θ, ϕ) and natural units, the metric

$$ds^2 = -\left(1 - \frac{r_s}{r}\right) dt^2 + \left(1 - \frac{r_s}{r}\right)^{-1} dr^2 + r^2 d\theta^2 + r^2 \sin^2\theta d\phi^2, \qquad (2.1)$$

where $r_s = 2MG$ is the Schwarzschild radius. If you look closely, the metric at $r = r_s$ and $r = 0$ exhibits singularities. However, coordinates are ways of labeling events in spacetime and so it is not necessary to give much importance to what values they will have (and if these values correspond to a singularity). Curvature, as a general criterion (we will not go into deep details) is measured by the Riemann tensor; despite this, it is difficult to determine when a tensor becomes infinite, since the components depend on the coordinates. But some scalars can be found by curvature and, since they are independent of the coordinates, it can be determined whether they are infinite or not. The simplest scalar is the Ricci scalar $R = g_{\mu\nu}R^{\mu\nu}$, but different types of higher-order scalars can be constructed, such as $R^{\mu\nu}R_{\mu\nu}$, $R^{\mu\nu\sigma\rho}R_{\mu\nu\sigma\rho}$, among others. If some of these scalars, but not necessarily all, are singular at a specific point, we say that this point is a curvature singularity. The point must also be at a finite distance from the curve; it cannot be an infinitely far point. In the case of the Schwarzschild metric, it suffices to observe that, with a direct calculation, we have

$$R^{\mu\nu\rho\sigma}R_{\mu\nu\rho\sigma} = \frac{48}{r^6}\left(GM\right)^2 \tag{2.2}$$

This contraction is crucial to conclude that r_s is just a singularity of the coordinates and that $r = 0$ is a singularity of the geometry of the system. In what follows, we will focus on the study of objects that are described by the Schwarzschild solution, even at radii smaller than r_s (what we colloquially call a black hole).

To study the geometry of a spacetime, we often examine the causal structure defined by the light cones. Consider the null radial curves, which are defined by

taking θ and ϕ constant and $ds^2 = 0$. For our metric, we then observe,

$$ds^2 = -\left(1 - \frac{2GM}{r}\right)dt^2 + \left(1 - \frac{2GM}{r}\right)^{-1}dr^2 = 0, \tag{2.3}$$

arriving at

$$\frac{dt}{dr} = \pm\left(1 - \frac{r_s}{r}\right). \tag{2.4}$$

This equation describes the slope of light cones in a $t - r$ spacetime diagram. As we approach $r = r_s$ we observe that the slope becomes $\pm\infty$ and thus the light cones are closing; see Fig. (2.1). This means that firstly the null geodesic seems to never pass r_s and secondly a distant observer seeing someone falling into the black hole will measure an infinite time (or equivalently, we will see that the intrepid astronaut will move slower and slower).

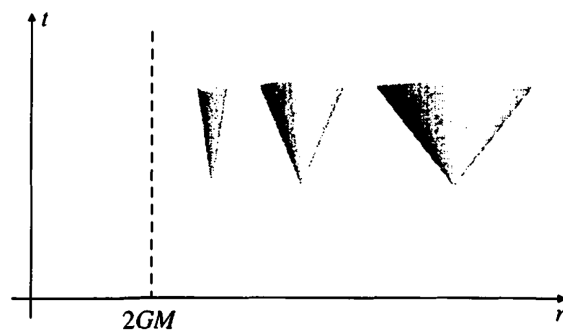Figure 2.1: Space-time diagram in Schwarzschild coordinates (t, r). The light cones are closing as we approach r_s. The diagram was taken from [12].

Since r_s is not formally a singularity in the geometry (again, a singularity in the coordinates), we can realize that the fact that the trajectory never reaches r_s is only due to the coordinates used. As a more optimal candidate for the coordinates, we

will use ones with which time moves more slowly along the null geodesics, called turtle coordinates and defined as follows:

$$t = \pm r + r_s \ln \left| \frac{r}{r_s} - 1 \right|. \tag{2.5}$$

Replacing this coordinate in the Schwarzschild metric, we arrive at

$$ds^2 = \left(1 - \frac{r_s}{r} \right) \left(-dt^2 + dr^{*2} \right) + r^2 d\theta^2 + r^2 \sin^2\theta d\phi^2. \tag{2.6}$$

At coordinates (t, r_*), the light cones no longer close as we approach the event horizon r_s, in contrast to what happens at (t, r). This is because the coordinate transformation relocates r_s to $r_* \to -\infty$, removing an apparent singularity; see Fig. (2.2).
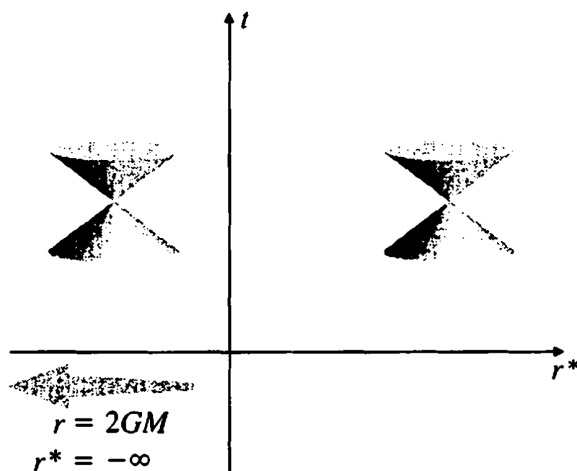

Figure 2.2: Diagram of spacetime in Schwarzschild coordinates (t, r^*). The light cones no longer close. The surface rs is now at infinity at r^*. The diagram was taken from [12].

While the above coordinate system moves r_s to infinity, we are interested in

finding a coordinate system where there is no problem in r_s without having to send it to infinity. Our next step is therefore to define the coordinates that align with the null geodesics. We say that

$$v = t + r^*$$
(2.7)

$$u = t - r^*,$$
(2.8)

with $v = cte$, characterizing the ingoing radial null geodesics and $u = cte$, characterizing the outgoing radial null geodesics. These coordinates are called Eddington-Finkelstein coordinates. The metric in terms of the coordinates v looks like

$$ds^2 = -\left(1 - \frac{r_s}{r}\right)dv^2 + (dvdr + drdv) + r^2d\theta^2 + r^2\sin\theta d\phi^2.$$
(2.9)

The surface r_s is no longer a problem (as we have said). The condition for radial curves is now

$$\frac{dv}{dr} = 0 \text{ (infalling)}$$
(2.10)

$$\frac{dv}{dr} = 2\left(1 - \frac{r_s}{r}\right) \text{ (outgoing)}$$
(2.11)

Light cones at these coordinates behave well when they reach r_s; see Fig. (2.3). The fact that they do not close does not mean that they do not tilt (as we see in the diagram). This implies that for $r < r_s$ all null trajectories directed into the future will be in the direction of decreasing r [12].

The surface r_s is known as the Schwarzschild event horizon. It is a surface of no return where no particle can return. A black hole is simply a region of space-time separated from infinity by an event horizon [12]. Since nothing escapes the event
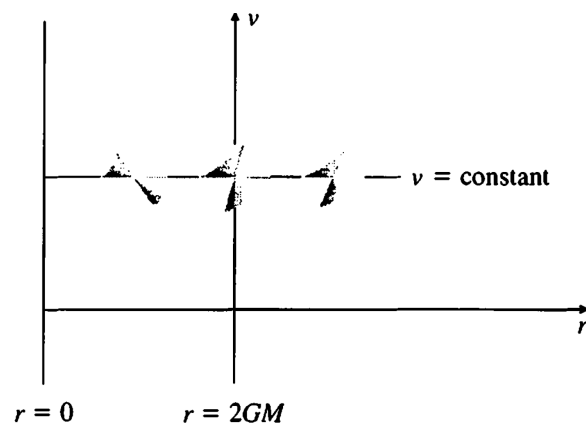
Figure 2.3: Diagram of spacetime in Schwarzschild coordinates (v, r). The light cones no longer close, but tilted as they pass through r_s. The surface rs is now in a finite position. The diagram was taken from [12].

horizon, we will not be able to see the interior of this object; hence the name black hole. The Schwarzschild solution can be extended maximally (see Chapter 5 of [12]), however, for the purposes of this work, the above description is sufficient.

2.2 The Geodesic Equation

If we have already established the geometry of spacetime (e.g., in the previous chapter the Schwarzschild metric), it is essential to study the motion of particles in such an environment. In general relativity, particles moving under the influence of the geometry of spacetime, with no external forces present, follow trajectories known as geodesics. These trajectories are determined by the geodesic equation, which is a crucial tool for describing the motion of particles in curved spacetimes. In this section, we will derive the geodesic equation, laying the groundwork for its use in later sections of this thesis.

Let us take the action for a massive particle, free from external forces, in a curved space-time:

$$S = m \int d\lambda \sqrt{-g(u,u)}, \tag{2.12}$$

where we will use the simplified notation instead of the component notation; i.e., $g(u,u) = g_{\mu\nu}u^{\mu}u^{\nu}$ and $\nabla_{\eta} = \eta^{\mu}\nabla_{\mu}$. Now consider a curve C that will represent a possible trajectory of the particle (see Fig. (2.4)). This curve is parameterized by the parameters τ and λ. At a certain point on the curve, we define the tangent vector $u = \partial/\partial t$ and the normal vector $\eta = \partial/\partial\lambda$ (separation vector between adjacent trajectories). The next step is to apply the principle of least action. This principle states that the trajectory followed by the particle is such that the action is stationary with respect to small variations of the trajectory. That is, we look for the paths for which the variation of the action is zero. To do this, we vary the action with respect to η:

$$\delta S = 0 \rightarrow \delta\left(\sqrt{-g(u,u)}\right) \equiv -\frac{m}{2\sqrt{-g(u,u)}}\nabla_{\eta}g(u,u) = -\frac{m}{2\sqrt{-g(u,u)}}\left[g(\nabla_{\eta}u,u) + g(u,\nabla_{\eta}u)\right]$$

$$= -\frac{m}{\sqrt{-g(u,u)}}\left[g(\nabla_{\eta}u,u)\right] = 0. \tag{2.13}$$

We have used the fact that the connection ∇ is that of Levi Chivita, which implies the compatibility of the metric $(\nabla_{\eta}g) = 0$ and that we have free torsion, that is, $\nabla_{u}\eta - \nabla_{\eta}u = [u,\eta]$. Since the vectors u and η are defined, the commutator (Lie bracket) $[u,\eta] = 0$; proving:

$$\nabla_{u}\eta = \nabla_{\eta}u. \tag{2.14}$$
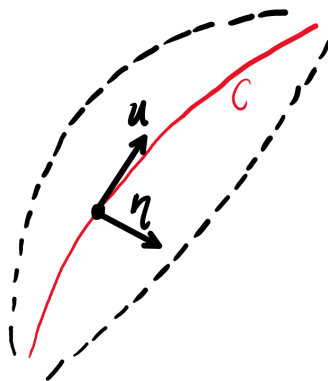
Figure 2.4: Possible trajectories of a particle with fixed endpoints. At a point in $C(\tau, \lambda)$ a tangent vector u and a normal vector η are established.

Then (2.13) now reads as

$$g(\nabla_\eta u, u) = g(\nabla_u \delta, u) = 0. \tag{2.15}$$

Integrating by parts:

$$\nabla_u g(\eta, u) - g(\eta, \nabla_u u) = 0 \tag{2.16}$$

The total derivative term $(\nabla_u g(\eta, u))$ is zero since at the extremes $\eta = 0$, then

$$g(\eta, \nabla_u u) = 0. \tag{2.17}$$

With η arbitrary, we conclude

$$g(\eta, \nabla_u u) = 0 \rightarrow \nabla_u u = 0. \tag{2.18}$$

The equation (2.18) is the equation of the geodesic. If a tangent vector u satisfies

this equation, it means that the integral curves of u are geodesics. Its relevance in this thesis is very important and we will use it in the next chapter. It should be noted that non-massive particles are also described by the geodesic equation. Its proof is similar, but with a slight change in the Lagrangian

2.3 $3+1$ Split of Spacetime

Einstein's equations, written entirely in covariant form, have the peculiarity that there is no clear distinction between space and time. There are situations where such a distinction is desirable, such as in a system where the dynamical evolution of a gravitational field in "time" is considered. The main approach to separating Einstein's field equations, in a way that allows us to introduce initial data and obtain in turn the evolution of the gravitational field, is the 3+1 formalism, which divides space-time into three-dimensional space and time.

To obtain the evolution of a physical system, one must formally generate this as an initial value or Cauchy problem. If we try to write Einstein's field equations as a Cauchy problem, we realize they are written in such a way that space and time are treated identically (which does not allow us to make a clear distinction). Therefore, we must create this distinction starting from the metric $g_{\alpha\mu}$. We must assume globally hyperbolic spacetimes; in other words, spacetimes that have a Cauchy surface. These spacetimes can be completely foliated, meaning they can be sliced into three-dimensional slices, making each three-dimensional slice spatial; see Fig. (2.5). Foliation can be interpreted as a set of levels of a parameter t, considered a function of universal time (which does not necessarily coincide with the proper time of a
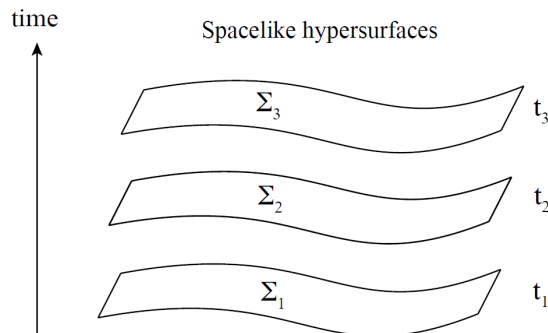
Figure 2.5: Space-time foliation. Each slice is a three-dimensional space-like hypersurface. The diagram was taken from [13].

particular observer).

Let us consider, for the moment, the example of a particular foliation and take two hypersurfaces Σ_t and Σ_{t+dt}. If we want the geometric information contained between these two hypersurfaces, we need (see Fig. (2.6)) [13]:

* The three-dimensional metric γ_{ij} that measures the proper distances within the hypersurface itself is:

$$dl^2 = \gamma_{ij}dx^idx^j. \tag{2.19}$$

* The lapse of proper time $d\tau$ between hypersurfaces (measured by observers moving along the normal direction to the hypersurface; also called Eulerian observers) is [13]:

$$d\tau = \alpha(t, x^i)dt, \tag{2.20}$$

α is the lapse function.

* The relative velocity β_i between Eulerian observers and constant spatial coor-
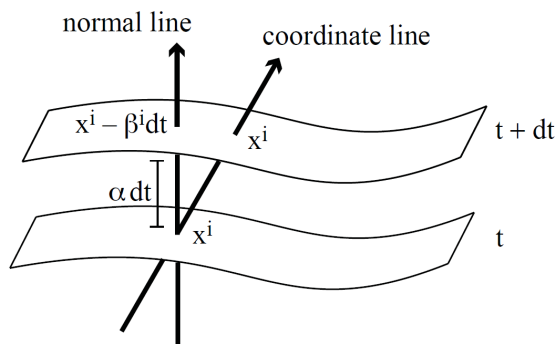
Figure 2.6: Two spatial hypersurfaces. The definition of the lapse function α and the shift vector β_i are graphically shown. The diagram was taken from [13].

dinates is related as:

$$x_{t+dt}^t = x_t^i - \beta^i(t, x^j)dt, \tag{2.21}$$

β_i being the displacement vector.

In terms of the functions $(\alpha, \beta_i, \gamma_{ij})$, the space-time metric takes the form

$$ds^2 = \left(-\alpha^2 + \beta_i \beta^i\right) dt^2 + 2\beta_i dt dx^i + \gamma_{ij} dx^i dx^j, \tag{2.22}$$

with $\beta_i = \gamma_{ij}\beta^j$ (the spatial metric raises or lowers indices). This equation is known as the 3 + 1 division of the metric. Note that

$$g_{\mu\nu} = \begin{pmatrix} -\alpha^2 + \beta_k \beta^k & \beta_i \\ \beta_j & \gamma_{ij} \end{pmatrix}, \tag{2.23}$$

and

$$g^{\mu\nu} = \begin{pmatrix} -1/\alpha^2 & \beta^i/\alpha^2 \\ \beta^j/\alpha^2 & \gamma^{ij} - \beta^i \beta^j/\alpha^2 \end{pmatrix}. \tag{2.24}$$

From these expressions it can be shown that the four-dimensional volume element can now be written as

$$\sqrt{-g} = \alpha\sqrt{\gamma} \tag{2.25}$$

where g and γ are the determinants of g_μ and γ_{ij}.

This decomposition of spacetime is extremely useful for this thesis (as will be seen in Chapter 4). Therefore, as a complement to the text, we will apply the decomposition in order to obtain the most fundamental equation of general relativity, the Einstein field equation, but now in the $3 + 1$ decomposition. To achieve this, we will discuss normal vectors to hypersurfaces, the projection operator, intrinsic and extrinsic curvature, and finally the Einstein field equation. This will not be a complete derivation, but we will reflect the main ideas of how to arrive at the field equation.

Consider a unit normal vector n^μ to the spatial hypersurfaces. This vector can be written in terms of the shift vector and the lapse function

$$n^\mu = \left(\frac{1}{\alpha}, -\frac{\beta^i}{\alpha}\right), \ n_\mu = (-\alpha, 0), \tag{2.26}$$

normal vector being, by definition, the 4-velocity of the Eulerian observers. It is possible to construct quantities in the $3 + 1$ formalism using the normal vector and such quantities do not depend on the choice of a coordinate system. Consider the global time function t, from which some things can be discovered. The lapse function is precisely defined in terms of t as $\alpha = (-\nabla t \cdot \nabla t)^{-1/2}$, and with this, the normal

vector n^μ is written in terms of t:

$$n^\mu = -\alpha \nabla^\mu t. \tag{2.27}$$

For the vector β^i three scalar functions β^i are introduced, such that if we move from one hypersurface to another following a normal direction, the change in coordinates is given by $x^i_{t+dt} = x^i_t - \beta^i dt$ and and it is easy to find

$$\beta^i = -\alpha \left(\vec{n} \cdot \nabla x^i \right). \tag{2.28}$$

A 4-vector (where we will use the notation $\vec{\beta}$ to refer to 4-vectors) $\beta^\mu = (0, \beta^i)$ can be constructed and it will be orthogonal to $\vec{n}$. From the latter and from $\vec{n}$, a temporal vector is also born, namely $t^\mu = \alpha n^\mu + \beta^\mu$, which is the tangent vector to the time lines (lines of constant spatial coordinates). Using t^μ, we will have

$$\beta_\mu = \gamma_{\mu\nu} t^\nu, \tag{2.29}$$

so the shift is the projection of the vector $\vec{t}$ on the spatial hypersurface. We conclude, meanwhile, that both the lapse function and the displacement are completely independent of the coordinates and are rather defined by the vector field $\vec{t}$.

All the magnitudes encountered above are not in vain, they are necessary to formulate Einstein's equations in the $3+1$ analysis. Before that, it is relevant to discuss curvature. In the $3+1$ decomposition, the intrinsic curvature, measured by the Riemann tensor associated to the spatial metric γ_{ij}, describes the internal

geometry of the spatial hypersurfaces. On the other hand, the extrinsic curvature, measured by the tensor $K_{\mu\nu}$, describes how these hypersurfaces are embedded or bent in spacetime. The tensor $K_{\mu\nu}$ can also be seen as a measure of the parallel transport performed on a normal vector on a hypersurface. Both magnitudes are essential to project Einstein's equations onto $3+1$ and to analyze the dynamics of the system.

To define the extrinsic curvature, we first define the projection operator on a spatial hypersurface, which is

$$P^\alpha_\beta = \delta^\alpha_\beta + n^\alpha n_\beta. \qquad (2.30)$$

The projection operator is used to project any spacetime tensor onto the spatial hypersurfaces of the 3+1 decomposition. With it we define the extrinsic curvature tensor:

$$K_{\mu\nu} = -P^\alpha_\mu \nabla_\alpha n_\nu = -\left(\nabla_\mu n_\nu + n_\mu n^\alpha \nabla_\alpha n_\nu\right). \qquad (2.31)$$

This tensor is purely spatial, which implies that its components $K^{00} = K^{0i} = 0$ (this also explains why the literature typically focuses only on the spatial components of the tensor). Another feature of the tensor is revealed by how it can be expressed using the Lie derivative. Note that, on the one hand, the spatial metric in the $3+1$ decomposition is defined as the metric induced on each hypersurface by the spacetime metric $g_{\mu\nu}$, in the form $\gamma_{\mu\nu} = g_{\mu\nu} + n_\mu n_\nu$. On the other hand, since n^α is unitary and normal, it satisfies $n^\alpha \nabla n_\alpha = 0$. If we apply the Lie derivative in the normal direction to the metric $\gamma_{\mu\nu}$ and use the two features mentioned above (on the metric

and the unit vector), we obtain:

$$
\begin{aligned}
\mathcal{L}_{\vec{n}}\gamma^{\mu\nu} &= n^\alpha \nabla_\alpha \gamma_{\mu\nu} + \gamma_{\mu\alpha}\nabla_\nu n^\alpha \\
&= n^\alpha \nabla_\alpha \left(g_{\mu\nu} + n_\mu n_\nu\right) + \left(g_{\mu\alpha} + n_\mu n_\alpha\right)\nabla_\nu n^\alpha + \left(g_{\nu\alpha} + n_\nu n_\mu\right)\nabla_\mu n^\alpha \\
&= n^\alpha \left(\nabla_\alpha n_\mu\right) n_\nu + n^\alpha n_\mu \left(\nabla_\alpha n_\nu\right) + \nabla_\nu n_\mu + \nabla_\mu n_\nu \\
&= \left(\gamma_\nu^\alpha - g_\nu^\alpha\right)\nabla_\alpha n_\mu + \left(\gamma_\mu^\alpha - g_\mu^\alpha\right)\nabla_\alpha g_\nu + \nabla_\nu n_\mu + \nabla_\mu n_\nu \\
&= \gamma_\nu^\alpha \nabla_\alpha n_\mu + \gamma_\mu^\alpha \nabla_\alpha n_\nu \\
&= -2K_{\mu\nu},
\end{aligned}
\tag{2.32}
$$

concluding that

$$
K_{\mu\nu} = -\frac{1}{2}\mathcal{L}_{\vec{n}}\gamma^{\mu\nu}.
\tag{2.33}
$$

Since n is normal to the hypersurface, for any scalar function ϕ, the equation (2.32) is rewritten in the form

$$
\mathcal{L}_{\vec{n}}\gamma_{\mu\nu} = \frac{1}{\phi}\mathcal{L}_{\phi\vec{n}}\gamma_{\mu\nu}.
\tag{2.34}
$$

If we select $\phi = \alpha$ (the lapse function):

$$
\left(\mathcal{L}_{\vec{t}} - \mathcal{L}_{\vec{\beta}}\right)\gamma_{\mu\nu} = -2\alpha K_{\mu\nu}.
\tag{2.35}
$$

Restricting ourselves to the spatial components and given that in the system studied $\mathcal{L}_{\vec{t}} = \partial_t$, we arrive at an equation of motion for the spatial metric γ_{ij}:

$$
\partial_t \gamma_{ij} = -2\alpha K_{ij} + D_i\beta_j + D_j\beta_i,
\tag{2.36}
$$

with D_i being the three-dimensional covariant derivative associated with γ_{ij}.

As already mentioned, our goal is to derive the Einstein field equations. The dynamics of the gravitational field is contained in these equations. In order to fit them to the 3+1 formalism, it is necessary to rewrite them in terms of intrinsic and extrinsic magnitudes associated to the spatial hypersurfaces. This process is carried out by contractions with the normal vector and the projection operator, thus separating the spatial and temporal contributions, and the final result is that the Einstein field equations will now be 2 constraint equations (giving us 4 field equations) and 2 evolution equations (giving us 6 field equations). As a starting point, the Riemann curvature tensor $R^{\alpha}_{\beta\mu\nu}$ of the spacetime is decomposed into the three-dimensional intrinsic curvature tensor $^{(3)}R^{\alpha}_{\beta\mu\nu}$ of the hypersurface and the extrinsic curvature tensor $K_{\mu\nu}$. This decomposition leads to the Gauss-Codazzi equations; which establish the relationship between the intrinsic and extrinsic geometry of the hypersurface, defined as [13]

$$P^{\delta}_{\alpha}P^{\beta}_{\kappa}P^{\mu}_{\lambda}P^{\nu}_{\sigma}R_{\sigma\kappa\lambda\sigma} = {}^{(3)}R^{\alpha}_{\beta\mu\nu} + K_{\alpha\mu}K_{\beta\nu} - K_{\alpha\nu}K_{\beta\mu}. \tag{2.37}$$

Now, the equation (2.37) implies that

$$P^{\alpha\mu}P^{\beta\nu}R_{\alpha\beta\mu\nu} = {}^{(3)}R + K^2 - K_{\mu\nu}K^{\mu\nu}, \tag{2.38}$$

with $K = K_\mu^\mu$. On the other hand, note that

$$P^{\alpha\mu}P^{\beta\nu}R_{\alpha\beta\mu\nu} = \left(g^{\alpha\mu} + n^\alpha n^\mu\right)\left(g^{\beta\nu} + n^\beta n^\nu\right)R_{\alpha\beta\mu\nu}$$

$$=R + 2n^\mu n^\nu R_{\mu\nu} \tag{2.39}$$

$$=2n^\mu n^\nu G_{\mu\nu},$$

being $G_{\mu\nu}$ the Einstein tensor. If we equate (2.38) and (2.39), and explicitly replace the Einstein tensor in terms of the energy momentum tensor; namely $G_{\mu\nu} = 8\pi T_{\mu\nu}$, we find a restriction called the Hamiltonian or energy restriction:

$$^{(3)}R + K^2 - K_{\mu\nu}K^{\mu\nu} = 16\pi n^\mu n^\nu T_{\mu\nu} = 16\pi\rho. \tag{2.40}$$

The other restriction arises from applying the mixed contraction of the Einstein tensor together with $P^{\alpha\nu}$ and n^ν in the the Codazzi-Mainardi equations [13]

$$P_\alpha^\delta P_\beta^\kappa P_\mu^\lambda n^\nu R_{\delta\kappa\lambda\nu} = D_\beta K_{\alpha\mu} - D_\alpha K_{\beta\mu}, \tag{2.41}$$

obtaining a constraint equation called the momentum constraint:

$$D_\mu\left(K^{\alpha\mu} - \gamma^{\alpha\mu}K\right) = -8\pi P^{\alpha^\mu} n^\nu T_{\mu\nu} = 8\pi j^\alpha. \tag{2.42}$$

The Hamilton and momentum constraints are conditions that must be met on each hypersurface, but they do not directly dictate how the geometry evolves. To find the evolution we must use the Codazzi-Mainardi equation, which together with the projection onto the hypersurface of the contracted Riemann tensor with the normal

vector [13]

$$P_\mu^\delta P_\nu^\kappa n^\lambda n^\sigma R_{\delta\lambda\kappa\sigma} = \mathcal{L}_{\vec{n}} K_{\mu\nu} + K_{\mu\lambda} K_\nu^\lambda + \frac{1}{\alpha} D_\mu D_\nu \alpha, \tag{2.43}$$

which brings us to

$$\partial_t K_{\mu\nu} = \mathcal{L}_{\vec{\beta}} K_{\mu\nu} - D_\mu D_\nu \alpha + \alpha \left[{}^{(3)}R_{\mu\nu} + K K_{\mu\nu} - 2K_{\mu\lambda} K_\nu^\lambda \right] + 4\pi\alpha \left[\gamma_{\mu\nu}(S - \rho) - 2S_{\mu\nu} \right], \tag{2.44}$$

defining $S_{\mu\nu} = P_\mu^\alpha P_\nu^\beta T_{\alpha\beta}$ and $S = S_\mu^\mu$. This equation, together with equation (2.36) dictate how γ_{ij} and $K_{\mu\nu}$ change with time, incorporating geometrical and matter contributions. The (2.36, 2.40, 2.42, 2.44) equations are then the rewriting of the Einstein Field equations in the $3 + 1$ decomposition, two constraint equations describing geometric and energetic relations on the hypersurface and two equations describing the evolution of the metric and the extrinsic curvature. These equations are fundamental for studying the dynamics of relativistic systems, since they allow general relativity to be formulated as an initial evolution problem, which is key in contexts such as the numerical simulation of black holes or gravitational waves.

Chapter 3

Stocastic Quantum Mechanics

Randomness is a central component of the description of quantum mechanics. It gives rise to alternative approaches for studying quantum mechanics, such as Stochastic Quantum Mechanics (SQM). Within this framework, quantum systems are considered to have an intrinsically random nature, allowing their properties to be analyzed from a probabilistic and dynamic perspective different from the conventional one [14]. SQM can be interpreted as a method that utilizes the information contained in the wave function and, through sampling of a stochastic process, constructs an equivalent description in terms of physical trajectories.

Nelson demonstrated that SQM is fundamentally equivalent to traditional quantum mechanics; see [14], but with a different approach that provides utility in developing new aspects of quantum theory, such as simulated trajectories of an electron in a hydrogen atom or a generalization of quantum field theory from a stochastic perspective; see [15]. On the other hand, the most fundamental hypothesis Nelson proposed to the theory is that every particle with mass m is subject to a stochastic process (a Brownian motion) with a diffusion coefficient $\sigma = \hbar/2m$. With this in

mind, it is possible to derive the Schrödinger equation, and it can also be shown that particles have trajectories that are continuous but not differentiable (due to the stochastic process). It should be noted that particles following stochastic processes, whether quantum or classical, follow their own dynamic rules; although SQM shares similarities, mathematically speaking, with Brownian motion, their dynamic descriptions are not the same.

The source of randomness in stochastic quantum mechanics has been a topic of ongoing debate. For example, Luis de la Peña and Ana María Cetto have approached this problem from the perspective of stochastic quantum electrodynamics, suggesting that the quantum behavior of particles results from their interaction with a background field known as the zero-point field (identified with the electromagnetic field), with the Planck constant being a measure of the magnitude of these fluctuations. Another approach, which we will adopt as a hypothesis in this thesis, suggests that space-time fluctuations act as a source of stochasticity. These ideas about the source of randomness inspire the development of the fundamental equations of stochastic quantum mechanics, both in flat spaces and in more complex geometries. Next, we will offer a first approximation to these equations in flat spaces, including the velocities and the dynamical equations of the system.

3.1 Basic Equations of Stochastic Quantum Mechanics

The way we approach stochastic quantum mechanics is similar to the theory proposed by Nelson. This mechanics is divided into kinematics and dynamics, where the evolution of the system is described by a Markovian process. The Langevin-

type differential equation describes the evolution of the process. This equation is asymmetric in time, since the process is not differentiable. The forward evolution in time $(+)$ and the backward evolution in time $(-)$ are determined by the Langevin equation

$$d\mathbf{x}_{\pm} = \mathbf{u}_{\pm}dt + \sqrt{2\sigma}dW_{\pm},\tag{3.1}$$

where

1. $\mathbf{u}_{\pm}$ are the forward and backward velocity fields.

2. $dW_{\pm}$ is the Wiener noise characterized by the properties:

$$\langle dW_{\pm}\rangle = 0,\tag{3.2}$$

$$\langle dW_{\pm i}dW_{\pm j}\rangle = \pm\delta_{ij}dt.\tag{3.3}$$

3. σ being the noise intensity (diffusion coefficient).

To find the dynamics of the system, we need to define appropriate differential operators for a stochastic function. Given the increments of dx (as a stochastic variable), it is possible to find the increments of any nonlinear function $y = f(x, t)$ by using the Taylor series expansion of that function and truncate it to second order (this procedure is known as Ito's formula); namely:

$$d_{\pm}y = \frac{\partial f}{\partial t}dt + \nabla f d\mathbf{x}_{\pm} + \frac{1}{2}\nabla^2 f \left(d\mathbf{x}_{\pm}\right)^2.\tag{3.4}$$

Replacing (3.1) in (3.4), we find:

$$
\begin{aligned}
d_{\pm} y &= \frac{\partial f}{\partial t} dt + \nabla f \left(\mathbf{u}_{\pm} dt + \sqrt{2\sigma} dW_{\pm} \right) + \frac{1}{2} \nabla^2 f \left(\mathbf{u}_{\pm} dt + \sqrt{2\sigma} dW_{\pm} \right)^2 \\
&= \left(\frac{\partial}{\partial t} + \mathbf{u}_{\pm} \cdot \nabla \right) f dt + \sqrt{2\sigma} \nabla f dW_{\pm} + \frac{1}{2} \nabla^2 f \left((\mathbf{u}_{\pm} dt)^2 + 2\sqrt{2\sigma} \mathbf{u}_{\pm} dt dW_{\pm} + 2\sigma \left(dW_{\pm} \right)^2 \right).
\end{aligned}
$$

$$(3.5)$$

If a term is of order $O(dt^2, dtdW, dW^3, \dots)$, its contribution in the infinitesimal limit is negligible compared to terms of order $O(dt, dW \text{ and } dW^2)$, then

$$
d_{\pm} y = \left(\frac{\partial}{\partial t} + \mathbf{u}_{\pm} \cdot \nabla \right) f dt + \sqrt{2\sigma} \nabla f dW_{\pm} + \sigma \nabla^2 f \left(dW_{\pm} \right)^2.
$$

$$(3.6)$$

Taking the average on both sides and using (3.2) and (3.3), we get

$$
\langle d_{\pm} y \rangle = \left(\frac{\partial}{\partial t} + \mathbf{u}_{\pm} \cdot \nabla \pm \sigma \nabla^2 \right) f dt.
$$

$$(3.7)$$

From equation (3.7), it is possible to define the forward derivative operator (D_+) and the backward derivative operator (D_-) as

$$
D_+ f = \left\langle \frac{d_+}{dt} f \right\rangle = \left(\frac{\partial}{\partial t} + \mathbf{u}_+ \cdot \nabla + \sigma \nabla^2 \right) f,
$$

$$(3.8)$$

$$
D_- f = \left\langle \frac{d_-}{dt} f \right\rangle = \left(\frac{\partial}{\partial t} + \mathbf{u}_- \cdot \nabla - \sigma \nabla^2 \right) f.
$$

$$(3.9)$$

The combinations that can be produced with both the velocity fields $\mathbf{u}_{\pm}$ and the derivative operators $D_{\pm}$ lead to the systematic velocities $\mathbf{v}$ and stochastic $\mathbf{u}$, and to the systematic derivative operators D_c and stochastic D_s; as defined by de la Peña

et al. in [10]:

$$\mathbf{v} = \frac{\mathbf{u}_+ + \mathbf{u}_-}{2}, \tag{3.10}$$

$$\mathbf{u} = \frac{\mathbf{u}_+ - \mathbf{u}_-}{2}, \tag{3.11}$$

$$D_c = \frac{D_+ + D_-}{2}, \tag{3.12}$$

$$D_s = \frac{D_+ - D_-}{2}. \tag{3.13}$$

Explicitly, the operators D_c and D_s can be written in terms of $\mathbf{v}$ and $\mathbf{u}$ using $D_\pm$:

$$D_c = \frac{\partial}{\partial t} + \mathbf{v} \cdot \nabla, \tag{3.14}$$

$$D_s = \mathbf{u} \cdot \nabla + \sigma \nabla^2. \tag{3.15}$$

Applying D_+, D_-, D_c y D_s to each component x_i, we derive that

$$D_+\mathbf{x} = \mathbf{u}_+, \ D_-\mathbf{x} = \mathbf{u}_-, \ D_c\mathbf{x} = \mathbf{v} \text{ y } D_s\mathbf{x} = \mathbf{u}. \tag{3.16}$$

Based on our current objective, which is to find the dynamics that describes the system, we will opt for the most general law and this implies, for example, that the relationship between accelerations and forces is linear. For this case we propose a total differential operator D of the form

$$D = D_c + \kappa D_s, \tag{3.17}$$

where κ is an arbitrary value. If we apply D to each component x_i, we can define a general velocity $\mathbf{w}$ such that

$$D\mathbf{x} = \mathbf{v} + \kappa\mathbf{u} = \mathbf{w}. \tag{3.18}$$

To determine the explicit form of the velocities and the value of κ we use the WKB approximation. This approximation follows a main motivation, and it is the connection between quantum mechanics and the hydrodynamic form of the Schrödinger equation, so we relate the wave function in its WKB form to the Madelung transformation for the wave function. The wave function in the WKB approximation is

$$\Phi = e^{i\mathcal{S}/\hbar}, \tag{3.19}$$

with $\mathcal{S}$ being a complex action. Since $\mathcal{S} = -i\hbar \ln\Phi$, it is possible to associate a complex velocity to this action, which is defined in the form [16]

$$\omega = \frac{\nabla\mathcal{S}}{m}, \tag{3.20}$$

m the mass of the particle.

The wave function can also be written in terms of the Madelung transformation, i.e.

$$\Phi = \sqrt{\rho}e^{(iS/\hbar)}, \tag{3.21}$$

$\rho = |\Phi|^2$ acting as the probability density and S being a real action. The relationship

between (3.19) and (3.21) is given by

$$\mathcal{S} = S - i\frac{\hbar}{2}\ln\Phi. \tag{3.22}$$

In this order of ideas, replacing this complex action in (3.20), we now have that

$$\omega = \mathbf{v} - i\mathbf{u}. \tag{3.23}$$

The values of the systematic velocity $\mathbf{v}$ and the stochastic velocity $\mathbf{u}$ are the same as those reported in [10]:

$$\mathbf{v} = \frac{\nabla S}{m}, \tag{3.24}$$

$$\mathbf{u} = \sigma\nabla\ln\left(\rho\right) = \frac{\hbar}{2m}\nabla\ln\left(\rho\right), \tag{3.25}$$

taking $\sigma = \hbar/2m$ as the diffusion coefficient which must be precisely that value to arrive at traditional quantum mechanics. If we compare (3.18) with (3.23), we realize that for the speeds to be equal, $\kappa = -i$; this value of the constant κ will be the one we will use in the remainder of the chapter.

The total acceleration of the system can easily be found by applying the general operator D to the velocity $\mathbf{w}$:

$$\mathbf{a} = D\mathbf{w} = (D_c - iD_s)(\mathbf{v} - i\mathbf{u}) = D_c\mathbf{v} - iD_c\mathbf{u} - iD_s\mathbf{v} - D_s\mathbf{u}. \tag{3.26}$$

Once we have found all the explicit forms for the velocities and differential operators we can obtain the forces acting on the particles. By expressing the total force f in

the form $f = f_+ + if_-$, where f_+ represents the components unchanged under time reversal and $f_{(-)}$ the components that reverse under time reversal—and assuming a linear dependence between forces and accelerations, it follows that the most general equations of motion, taking both their real and imaginary parts, are

$$m(D_c\mathbf{v} - D_s\mathbf{u}) = f_+, \tag{3.27}$$

$$-m(D_c\mathbf{u} + D_s\mathbf{v}) = f_-. \tag{3.28}$$

Let us consider the conservative problem. Suppose that $f = -\nabla V(x)$ (so $f_- = 0$). Equation (3.28) will now be

$$m(D_c\mathbf{u} + D_s\mathbf{v}) = 0. \tag{3.29}$$

Replacing the values of the differential operators, we arrive at

$$m\left[\frac{\partial \mathbf{u}}{\partial t} + (\mathbf{v} \cdot \nabla)\mathbf{u} - (\mathbf{u} \cdot \nabla)\mathbf{v} - \frac{\hbar}{2m}\nabla^2\mathbf{v}\right] = 0. \tag{3.30}$$

We decompose $\mathbf{v}$ and $\mathbf{u}$ as in (3.24) and (3.25)[1]. Using the gradient identity of a dot product for any vector $\mathbf{A}$ and $\mathbf{B}$:

$$\nabla(\mathbf{A} \cdot \mathbf{B}) = (\mathbf{A} \cdot \nabla)\mathbf{B} + (\mathbf{B} \cdot \nabla)\mathbf{A} + \mathbf{A} \times (\nabla \times \mathbf{B}) + \mathbf{B} \times (\nabla \times \mathbf{A}) \tag{3.31}$$

---

[1]I want to make a remark at this point. If we wanted to add information about possible rotational contributions of $\mathbf{v}$ we would have to add a term that gives us this information (such as a vector **b**). For the moment, and since this is a conservative problem, we reduce the description to the case $\nabla \times \mathbf{v} = 0$.

and equation (3.25), we find that (3.30) is now

$$\nabla \left[\frac{1}{\rho} \left(\frac{\partial \rho}{\partial t} + \nabla \cdot \rho \mathbf{v} \right) \right] = 0, \tag{3.32}$$

or

$$\left(\frac{\partial \rho}{\partial t} + \nabla \cdot \rho \mathbf{v} \right) = 0. \tag{3.33}$$

Equation (3.33) is the continuity equation that expresses the local conservation of particles.

On the other hand, for the equation (3.27) we have

$$m(D_c \mathbf{v} - D_s \mathbf{u}) = -\nabla V(x). \tag{3.34}$$

Replacing the derivative operators:

$$m \left[\frac{\partial \mathbf{v}}{\partial t} + (\mathbf{v} \cdot \nabla) \mathbf{v} - (\mathbf{u} \cdot \nabla) \mathbf{u} - \frac{\hbar}{2m} \nabla^2 \mathbf{u} \right] = -\nabla V. \tag{3.35}$$

Making use of vector identities

$$\frac{1}{2} \nabla \mathbf{A}^2 = (\mathbf{A} \cdot \nabla) \mathbf{A} + \mathbf{A} \times (\nabla \times \mathbf{A}),$$

$$\nabla^2 \mathbf{A} = \nabla(\nabla \cdot \mathbf{A}) - \nabla \times (\nabla \times \mathbf{A}),$$

and equations (3.24) and (3.25), it is possible to rewrite (3.35) in the following manner

$$\nabla \left[\frac{\partial S}{\partial t} + \frac{1}{2} m \mathbf{v}^2 + V_Q + V \right] = 0 \tag{3.36}$$

or

$$\frac{\partial S}{\partial t} + \frac{1}{2}m\mathbf{v}^2 + V_Q + V = 0, \tag{3.37}$$

being V_Q:

$$V_Q = -\left(\frac{1}{2}m\mathbf{u}^2 + \frac{\hbar}{2}\nabla \cdot \mathbf{u}\right) = -\frac{\hbar^2}{2m}\frac{\nabla^2\sqrt{\rho}}{\sqrt{\rho}}. \tag{3.38}$$

which is known as quantum potential. This last equation is a Hamilton-Jacobi-type equation modified by the quantum potential. Both, continuity equation and Hamilton-Jacobi equation are equivalent to the hydrodynamic representation of the Schrödinger equation [17].

Another peculiarity of our result is related to the Euler equation for a fluid, which is defined as

$$\frac{\partial \mathbf{v}}{\partial t} + \mathbf{v} \cdot \nabla \mathbf{v} = -\frac{\nabla p}{\rho} + \mathbf{g}, \tag{3.39}$$

with ρ the mass density, $\mathbf{u}$ the flow velocity, p is the mechanical pressure and f are the external forces. Then, by specifying $\mathbf{g} = -\nabla V$, it becomes clear that equation (3.37) (or better seen, equation (3.36) taking $\mathbf{v} = \nabla S/m$) is a Euler equation plus a quantum potential (the pressure term results from specifying the potential V). All this treatment carried out in this chapter will be used in the next chapter, where we will analyze stochastic quantum mechanics as seen from curved spaces.

Chapter 4

Stochastic Quantum Mechanics in Curved Spaces

The Klein-Gordon (KG) equation in curved spacetime describes the relativistic dynamics of scalar particles, such as charged bosons, under the influence of spacetime geometry. When reformulated in hydrodynamic terms, this equation translates the evolution of the scalar field into macroscopic variables such as particle density and current flow. This representation leads to an equivalent system of equations, consisting of a continuity equation and a Hamilton-Jacobi-like equation, which explicitly incorporate terms associated with the quantum potential and spacetime curvature.

On the other hand, stochastic quantum mechanics in curved spacetime (SQM-CS) models the motion of quantum particles as stochastic trajectories around geodesics, where spacetime fluctuations are treated as a source of randomness. These fluctuations can be interpreted as a background of gravitational waves that permeate spacetime and that, when colliding with particles, will cause their trajectories, which are normally described by geodesics according to general relativity, to become stochastic trajectories. This approach, based on stochastic differential equations, also allows for the derivation of the Klein-Gordon equation in its hydrodynamic form.

In this chapter, we will address two main topics. First, we will study the dynamics of a charged boson gas with arbitrary potential described by the Klein-Gordon-Maxwell equation (KGM), developing its hydrodynamic representation in curved spaces, and describing how its decomposition into density and phase gives rise to a continuity equation and a Hamilton-Jacobi type equation. Second, we will explore how SQM-CS, through stochastic processes that take spacetime fluctuations as a source and a dynamic construction based on a simple relationship between accelerations and forces, leads to the same hydrodynamic equations of Klein-Gordon. This establishes a profound connection between spacetime quantum fluctuations and fundamental quantum equations [2].

4.1 Field Equations

We model a boson gas as a set of excitations of a scalar field with arbitrary potential that is minimally coupled to a gauge vector field through electromagnetic interaction and described by the KGM [18]. Our goal for this section is to extend the KGM equations using coordinates in a four-dimensional manifold that acts as the curved physical spacetime, whose geometry is determined by a metric g. For the remainder of this section, we will use natural units, that is, $c = \hbar = \epsilon_0 = \mu_0 = 1$. The d'Alembert operator of interest in our case is of the form:

$$\Box_E = \left(\nabla^\mu + ieA^\mu \right) \left(\nabla_\mu + ieA_\mu \right). \tag{4.1}$$

with e the charge of the particle and A_μ the gauge vector field associated with the Maxwell $4-$potential. Therefore, the KGM equations, which come from a Lagrangian density that is invariant under transformations of the $U(1)$ group, are written as

$$\Box_E \Phi - \frac{dV}{d\Phi} = 0, \tag{4.2}$$

$$\nabla_\nu F^{\mu\nu} = J^{E\mu}, \tag{4.3}$$

where $\Phi(t, x)$ is a complex scalar field, $F_{\mu\nu} = \nabla_\mu A_\nu - \nabla_\nu A_\mu$ is the Faraday tensor, V an arbitrary potential and J_μ^E is the conserved 4-current

$$J_\mu^E \equiv i \frac{e}{2m^2} \left[\Phi \left(\nabla_\mu - ieA_\mu \right) \Phi^* - \Phi^* \left(\nabla_\mu + ieA_\mu \right) \Phi \right]. \tag{4.4}$$

We use the $3+1$ decomposition for the metric (see subsection (2.3)), which means that we divide the four-dimensional spacetime into three spatial dimensions and one temporal dimension. The three spatial dimensions form three-dimensional hypersurfaces, whereas the temporal dimension, represented by the parameter t, describes the evolution of these hypersurfaces over time. This decomposition allows to study spacetime in terms of its spatial geometry and temporal dynamics, hence the name $3+1$. The metric is given by

$$ds^2 = -N^2 dt^2 + \gamma_{ij} \left(dx^i + N^i dt \right) \left(dx^j + N^j dt \right), \tag{4.5}$$

γ_{ij} being the spatial metric, $N(t, x^i)$ the lapse function, and $N^i(t, x^j)$ the shift vector[1].

---

[1]It is worth noting that we are using a different kind of notation for the lapse function and the shift vector compared to (2.22). But it is completely equivalent, since $\alpha = N$ and $\beta_i = N^i$.

A remarkable property of the Klein-Gordon equation is its admittance of localized and non-dispersive solutions under certain conditions, which is especially relevant in physical processes such as scattering. However, Derrick's theorem states that in a flat spacetime, scalar field solutions that are static and localized turn out to be unstable. This limitation can be overcome by introducing a harmonic decomposition of the complex scalar field, where the time dependence is included in a phase factor, such that Φ looks like

$$\Phi(x^0, \mathbf{x}) = \Psi(x^0, \mathbf{x})e^{-i\omega_0 x^0}. \tag{4.6}$$

where ω_0 is the particle mass or the frequency for massless particles, Ψ is an amplitude, and $n(t, \mathbf{x}) = |\Phi|^2 = |\Psi|^2$ is the particle density. This approach breaks the staticity of the field, while spacetime remains static, allowing the existence of soliton-like solutions [19, 20].

We will use the hydrodynamic representation to express the field equations derived from KGM. Recall that Madelung introduced the hydrodynamic representation of Schrödinger (see [17]). He showed that it is equivalent to an Euler equation for an irrotational fluid, adding a quantum potential (as we mentioned in the previous chapter, see equation (3.37)). The boson gas can be viewed as a real fluid, which is described by quantum Euler equations [18]. Then, for our case, the solution (4.6) can be decomposed into its hydrodynamic form by taking the amplitude Ψ as the Madelung transformation ($x^0 = t$, the time coordinate)

$$\Psi(t, \mathbf{x}) = \sqrt{n(t, \mathbf{x})}e^{iS}, \tag{4.7}$$

finding that $\Phi(t, \mathbf{x})$ now takes the form

$$\Phi(t, x) = \sqrt{n}e^{i\theta} = \sqrt{n}e^{i(S-\omega_0 t)}. \tag{4.8}$$

The complex scalar field has been decomposed into a density $n(t, x)$ and a phase $\theta(t, x) = S(t, \mathbf{x}) - \omega_0 t$ ($S(t, \mathbf{x})$ contains the information about the geometry of the system). This decomposition allows us to define the generalized velocity π^μ:

$$\pi^\mu = \frac{1}{m}\left(\nabla^\mu\theta + eA^\mu\right) = v^\mu - \frac{\omega_0}{m}\nabla^\mu t, \tag{4.9}$$

m being the mass of the particle and the velocity of an individual particle is taken as[2]

$$v^\mu = \frac{1}{m}\left(\nabla^\mu S + eA^\mu\right). \tag{4.10}$$

If we replace the solution Φ (4.8) and the individual velocity v^μ (4.10) in (4.2), we find two types of equations (in particular, their imaginary and real parts), the continuity equation

$$\nabla^\mu(nv_\mu) - \frac{\omega_0}{m}(\nabla^0 n + n\Box t) = 0, \tag{4.11}$$

and the Hamilton-Jacobi equation

$$v_\mu v^\mu - 2\frac{\omega_0}{m}v^0 - \frac{\omega_0^2}{m^2 N^2} + \mathcal{A} - V_Q = 0, \tag{4.12}$$

identifying $V_Q = \dfrac{\Box\sqrt{n}}{m^2\sqrt{n}}$ as a quantum potential and $\mathcal{A}$ a variable containing an ar-

---

[2]v^μ is not a unit normal 4-vector, i.e. in our case $v_\mu v^\mu = 1$ is not true.

bitrary self-interacting potential which we conveniently write as $\mathcal{A} = \dfrac{V}{2m^2 n}$. Writing these last two equations in terms of the generalized velocity π_α and the density of n, we find

$$\nabla_\alpha(n\pi^\alpha) = 0 \tag{4.13}$$

and

$$\frac{1}{2}\pi_\alpha \pi^\alpha + \mathcal{A} - \frac{1}{2}V^Q = 0. \tag{4.14}$$

Equations (4.13) and (4.14) are the KG equation written in the variables π_α and n [2]. Now, as a new objective (which will be discussed in the following sections), we aim to use stochastic theory to derive these same equations.

4.2 Stochastic Quantum Mechanics in Curved Spaces

The assumptions considered to establish the stochastic mechanism in curved space-time are the following [2]:

1. Quantum particles interact with the stochastic background of spacetime, which is universally present. This interaction is analogous to Brownian motion in classical physics. It is not just a small perturbation, but is a fundamental aspect to describe quantum behavior.

2. The interaction between a quantum particle and the background radiation cannot be fully known in detail. Instead, only its statistical properties are considered, similar to the statistical properties governing Brownian motion.

To make sense of what has been described above, we will start with the stochastic differential equation that is associated with the 4-velocity

$$\frac{dx^\mu}{d\tau} = U^\mu + \sqrt{2\sigma}\xi^\mu(\tau), \tag{4.15}$$

with $U^\mu = dx^\mu/d\tau$ (the 4-velocity) and σ is the diffusion coefficient. Another way to write the equation is

$$dx^\mu = U^\mu d\tau + \sqrt{2\sigma}d\tilde{W}^\mu(\tau), \tag{4.16}$$

where $d\tilde{W}^\mu(\tau) = \xi^\mu(\tau)d\tau$ corresponds to the Wiener process[3] (note that in practice what we are doing is creating a coupling to a stochastic differential equation, where our "time" is now proper time; compare with equation (3.1)).

The way we are approaching the physical problem is in line with Nelson's non-relativistic approach. Initially, forward and backward stochastic differential equations are introduced, given the time reversibility. For our case, we introduce the forward $(+)$ and backward $(-)$ stochastic differential equations (see equation (4.16)) for the trajectory of a quantum particle in terms of its 4-velocity; that is

$$dx_+^\mu = U_+^\mu d\tau + \sqrt{2\sigma}d\tilde{W}_+^\mu(\tau), \tag{4.17}$$

$$dx_-^\mu = U_-^\mu d\tau + \sqrt{2\sigma}d\tilde{W}_-^\mu(\tau). \tag{4.18}$$

---

[3]In Chapter 3 we mentioned some properties of the Wiener process. In the particle frame, Ito's lemma tells us that $(dW(\tau))^2 = d\tau$ and for the metric (4.5) (3+1 foliation) we have $d\tau = N(t, x^i)dt$.

where $d\tilde{W}^{\mu}_+(\tau)$ and $d\tilde{W}^{\mu}_-(\tau)$ satisfy the properties of a Wiener process:

$$\langle d\tilde{W}^{\mu}_{\pm}(\tau)\rangle = 0, \text{ (zero mean value)} \tag{4.19}$$

$$\langle d\tilde{W}^{\mu}_{\pm}(\tau)d\tilde{W}^{\mu}_{\pm}(\tau')\rangle = \pm d\tau\delta(\tau - \tau')\delta^{\mu\nu}. \text{ (correlation function)} \tag{4.20}$$

The generalized velocity π^{μ} (forward average) and the stochastic velocity (backward average) u^{μ} can be defined as follows

$$\pi^{\mu} = \frac{U^{\mu}_+ + U^{\mu}_-}{2} \text{ and } u^{\mu} = \frac{U^{\mu}_+ - U^{\mu}_-}{2}. \tag{4.21}$$

The wave function Φ, in its WKB form, is expressed as

$$\Phi = e^{i\mathcal{S}}, \tag{4.22}$$

$\mathcal{S}$ being the complex action. Its complex velocity is represented as

$$w^{\mu} = \frac{\nabla^{\mu}\mathcal{S}}{m} = -\frac{i}{m}\nabla^{\mu}(\ln(\Phi)). \tag{4.23}$$

The relationship between $\mathcal{S}$ and the phase of (4.8) is:

$$\mathcal{S} = S - \omega_0 t - \frac{i}{2}\ln(n). \tag{4.24}$$

Then the velocity w^{μ} takes the form

$$w^{\mu} = \frac{\nabla^{\mu}S}{m} - \frac{\omega_0}{m}\nabla^{\mu}t - \frac{i}{2m}\nabla^{\mu}(\ln(n)). \tag{4.25}$$

Two velocities are observed (such velocities have been reported in [21, 22]). One that is clearly dependent on the phase S (and if there is an electromagnetic field, it can be associated with (4.9))

$$\pi^\mu = v^\mu - \frac{\omega_0}{m} \nabla^\mu t \tag{4.26}$$

and another dependent on n (called stochastic velocity)

$$u^\mu = \sigma \nabla(\ln(n)). \tag{4.27}$$

Here, $\sigma = \frac{1}{2m}$ in natural units or $\sigma = \frac{\hbar}{2m}$ in standard units, represent the diffusion coefficient. This value of σ, which was introduced by Nelson as part of his formulation of the quantum stochastic process and was already used in the previous chapter, will now be employed in the formulation for arbitrary spacetimes.

The velocity w^μ, which is a general velocity that encompasses both π^μ and u^μ, is written as

$$w^\mu = \pi^\mu - iu^\mu. \tag{4.28}$$

Given the general velocity, it is possible to find the equation of motion for stochastic particles by fixing the total acceleration

$$a^\mu \equiv \frac{dw^\mu}{d\tau} = 0, \tag{4.29}$$

However, since a stochastic differential equation is fulfilled, it is necessary to follow Ito's rule, or in other words, we will use the same dynamic arguments that we used in the previous chapter to find the respective time derivatives $\hat{\mathcal{D}}$, but now of

a generalized character for arbitrary curved spacetimes. Let's start, as we already know, by developing a Taylor series expansion to a function $g(x^\mu)$ and truncating it to second order:

$$dg(x^\mu) = \nabla_\mu g(x^\mu) dx^\mu + \frac{1}{2} \nabla_\mu \nabla^\mu (dx^\mu)^\mu. \tag{4.30}$$

Using the forward stochastic process of equation (4.17), we have that the expansion reduces (higher orders of $d\tau$ and $d\tilde{W}_+^\mu$ are zero)

$$dg(x^\mu) = U_+^\mu \nabla_\mu g(x^\mu) d\tau + \sqrt{2\sigma} \nabla_\mu g(x^\mu) d\tilde{W}_+^\mu + \sigma \left(d\tilde{W}_+^\mu \right)^2. \tag{4.31}$$

As we did in the previous chapter, it is possible to find the time derivative by averaging all possible events (differential average), which gives us the forward derivative[4]

$$\hat{\mathcal{D}}_+ g(x^\mu) = \left\langle \frac{d}{d\tau} g(x^\mu) \right\rangle = [U_+^\mu \nabla_\mu + \sigma \nabla_\mu \nabla^\mu] g(x^\mu). \tag{4.32}$$

In terms of π^μ and u^μ, we have

$$\hat{\mathcal{D}}_+ g(x^\mu) = [(\pi^\mu + u^\mu) \nabla_\mu + \sigma \nabla_\mu \nabla^\mu] g(x^\mu). \tag{4.33}$$

If we consider the opposite process (backwards, equation (4.18)), we find, in terms of π^μ and u^μ

$$\hat{\mathcal{D}}_- g(x^\mu) = [(\pi^\mu - u^\mu) \nabla_\mu + \sigma \nabla_\mu \nabla^\mu] g(x^\mu). \tag{4.34}$$

---

[4]We use the properties (4.19) and (4.20).

Adding the respective derivatives, we will arrive at the systematic derivative:

$$\hat{\mathcal{D}}_c = \frac{\hat{\mathcal{D}}_+ + \hat{\mathcal{D}}_-}{2} = \pi^\mu \nabla_\mu. \tag{4.35}$$

By subtracting we arrive at the stochastic derivative:

$$\hat{\mathcal{D}}_s = \frac{\hat{\mathcal{D}}_+ - \hat{\mathcal{D}}_-}{2} = u^\mu \nabla_\mu + \sigma \nabla^\mu \nabla_\mu. \tag{4.36}$$

All of the above is in agreement with what has already been done with time derivatives in the previous chapter. Since we are analyzing moving quantum particles, the spacetime regions adjacent to the particles are locally flat, which implies that if we apply x^μ to $\hat{\mathcal{D}}_c$ and $\hat{\mathcal{D}}_s$[5]:

$$\hat{\mathcal{D}}_c x^\mu = \pi^\mu \tag{4.37}$$

and

$$\hat{\mathcal{D}}_s x^\mu = u^\mu. \tag{4.38}$$

The next step in our recipe is to find the dynamics that describes the system. Let us remember that in the previous chapter we had mentioned the importance of creating the dynamics from a general law; that is, one where the accelerations and the forces are linear. To do this, we introduce, as in the previous chapter, a differential operator $\hat{\mathcal{D}}$ of the form

$$\hat{\mathcal{D}} = \hat{\mathcal{D}}_c + \kappa \hat{\mathcal{D}}_s, \tag{4.39}$$

---

[5]We use the fact that $\nabla_\nu x^\mu = \partial_\nu x^\mu \delta_\mu \delta^\nu$ in a locally flat coordinate system.

where κ is an arbitrary value. If we apply x^μ to $\hat{\mathcal{D}}$, we can define a general velocity w^μ such that

$$\hat{\mathcal{D}}x^\mu = \pi^\mu + \kappa u^\mu = \omega^\mu. \tag{4.40}$$

Comparing equation (4.40) with (4.28), it is observed that for both velocities to be equal $(w^\mu = \omega^\mu)$, consequently $\kappa = -i$.

The acceleration of the system is found by applying the differential operator $\hat{\mathcal{D}}$ with the velocity w^μ:

$$a^\mu = \hat{\mathcal{D}}w^\mu = (\hat{\mathcal{D}}_c - i\hat{\mathcal{D}}_s)(\pi^\mu - iu^\mu) = \hat{\mathcal{D}}_c\pi^\mu - \hat{\mathcal{D}}_s u^\mu - i(\hat{\mathcal{D}}_c u^\mu + \hat{\mathcal{D}}_s \pi^\mu). \tag{4.41}$$

We will use the following identity to explicitly obtain all the values of the differential operators applied to π^μ and u^μ:

$$\nabla_\alpha \pi^\mu = \nabla^\mu \pi_\alpha + \frac{e}{2m}F^\mu_\alpha = \nabla^\mu \pi_\alpha + 2e\sigma F^\mu_\alpha, \tag{4.42}$$

F^μ_α being the Maxwell tensor. So, it is easy to prove (for π^μ):

$$\hat{\mathcal{D}}_c\pi^\mu = \frac{1}{2}\nabla^\mu(\pi_\alpha \pi^\alpha) + 2\sigma e F^{\mu\alpha}\pi_\alpha, \tag{4.43}$$

$$\hat{\mathcal{D}}_s\pi^\mu = \sigma\left(\nabla^\mu \nabla_\alpha \pi^\alpha + \nabla_\alpha(\ln(n))\nabla^\mu \pi^\alpha\right) + 2\sigma^2 e \nabla_\alpha F^{\alpha\mu} + 2\sigma e F^{\mu\alpha}u_\alpha, \tag{4.44}$$

and (for u^μ)

$$\hat{\mathcal{D}}_c u^\mu = \sigma \pi_\alpha \nabla^\alpha \left(\frac{\nabla^\mu n}{n}\right), \tag{4.45}$$

$$\hat{\mathcal{D}}_s u^\mu = 2\sigma^2 \nabla^\mu \left(\frac{\Box \sqrt{n}}{\sqrt{n}} \right). \tag{4.46}$$

In particular, we note that if we neglect the stochastic behavior and the electromagnetic field in (4.43), we see [2]

$$\hat{\mathcal{D}}_c \pi^\mu = \pi_\alpha \nabla^\alpha \pi^\mu = \nabla_\pi \pi^\mu. \tag{4.47}$$

In the absence of forces ($\hat{\mathcal{D}}_c \pi^\mu = 0$), equation (4.47) becomes the definition of the vector π^α whose integral curve is the geodesic[6].

The total net force f^μ decomposes as $f^\mu = f_+^\mu + i f_-^\mu$. Taking the linearity between forces and accelerations, we have

$$ma^\mu = m \left(\hat{\mathcal{D}}_c \pi^\mu - \hat{\mathcal{D}}_s u^\mu \right) - im(\hat{\mathcal{D}}_c u^\mu + \hat{\mathcal{D}}_s \pi^\mu) = f_+ + i f_-, \tag{4.48}$$

or, the real and imaginary part ($f_+^\mu = F^\mu + F_E^\mu$)

$$m(\hat{\mathcal{D}}_c \pi^\mu - \hat{\mathcal{D}}_s u^\mu) = F^\mu + F_E^\mu, \tag{4.49}$$

$$-m(\hat{\mathcal{D}}_c u^\mu + \hat{\mathcal{D}}_s \pi^\mu) = f_-. \tag{4.50}$$

If we study a system with $F^\mu = -m\nabla^\mu \mathcal{A}$ being a conservative force that is associated with an arbitrary potential of the form $V = 2m^2 \mathcal{A} n$ and $F_E^\mu = 2\sigma m F^{\alpha\mu} \pi_\alpha$ is the

---

[6]When there is no stochastic contribution, we will only find classical geodesics; as expected.

Lorentz force, we find two equations:

$$\nabla^\mu \left[\frac{1}{2} \left(\pi_\alpha \pi^\alpha \right) - 2\sigma^2 \left(\frac{\Box \sqrt{n}}{\sqrt{n}} \right) + \mathcal{A} \right] = 0, \tag{4.51}$$

$$\nabla^\mu \left[\sigma \nabla_\alpha \pi^\alpha + u_\alpha \pi^\alpha \right] = f_- - 2\sigma^2 em \nabla_\alpha F^{\alpha\mu} - 2\sigma em F^{\mu\alpha} u_\alpha. \tag{4.52}$$

Integrating, individually, the term within the brackets in (4.51), we arrive at

$$\frac{1}{2} \pi_\alpha \pi^\alpha + \mathcal{A} + C - 2\sigma^2 \left(\frac{\Box \sqrt{n}}{\sqrt{n}} \right) = 0, \tag{4.53}$$

which again, is the equation (4.14) with an integration constant C. In equation (4.52) it is clear that the term inside the parentheses is precisely the continuity equation (4.13):

$$\sigma \nabla_\alpha \pi^\alpha + u_\alpha \pi^\alpha = 0. \tag{4.54}$$

Thus, the term in brackets disappears and implies that the force f_- acts as a diffusion force that changes with time reversal, fixing it to have the value

$$f_- = m(\sigma \nabla_\alpha F^{\alpha\mu} + u_\alpha F^{\mu\alpha}). \tag{4.55}$$

There is no doubt that the field equation of a quantum particle immersed in a fluctuating and arbitrarily curved spacetime is fully identified with the KG equation (equations (4.53) and (4.54), which is what we were hoping to get to!). It is also worth noting that Φ denotes a function whose main purpose is to describe the stochastic trajectory of a quantum particle under the influence of the environment, rather than

referring to a bosonic particle or a scalar field [2]. Also, something worth noting is that the quantum potential arises naturally from the purely stochastic contribution of the acceleration, i.e. from the $\hat{\mathcal{D}}_s u^\mu$ term. If we combine this term with the expression for $\hat{\mathcal{D}}_c \pi^\mu$, we find (in terms of velocity v^μ; see equation (4.26))

$$v_\mu \nabla^\mu v_\alpha - \frac{\omega_0}{m} \nabla^0 v_\alpha - \frac{\omega_0^2}{2m^2} \nabla_\alpha \left(\frac{1}{N^2} \right) - \frac{1}{2m^2} \nabla_\alpha \left(\frac{\Box \sqrt{n}}{\sqrt{n}} \right)$$
$$= -\nabla_\alpha \mathcal{A} - \frac{e}{m} \left(F_\alpha^\mu v_\mu - \frac{\omega_0}{m} F_\alpha^0 \right) \quad (4.56)$$

which is exactly the Euler equation reported in [18]. If integrated (4.56), we arrive at the Hamilton-Jacobi equation (4.12). Both equations (Euler's and Hamilton-Jacobi's) are related to each other and come from the hydrodynamic representation of the Klein-Gordon equation in a curved spacetime.

In the Newtonian limit, the continuity equation (4.54), or (4.11) which is written in terms of v^μ, reduces to

$$\partial_t n + \nabla \cdot (n\mathbf{v}) = 0 \quad (4.57)$$

This equation ensures the conservation of the probability density in flat spacetime and corresponds to the classical continuity equation modified by quantum effects, so it is clear that our work is a generalization to curved spaces. Taking into account the other acceleration terms, i.e. $\hat{\mathcal{D}}_s \pi^\mu$ and $\hat{\mathcal{D}}_c u^\mu$ (see equation (4.50)) we obtain the derivative of the continuity equation and the force terms f_-. It is important to mention that we identify precisely this equation as a restriction of the system instead of a dynamical relation.

The equation (4.56) can be rewritten as follows

$$v_\mu \nabla^\mu v_\alpha - \frac{\omega_0}{m} \nabla^0 v_\alpha = F_\alpha^E + F_\alpha^Q + F_\alpha^G + F_\alpha^n, \tag{4.58}$$

where, in the written order, we have the generalized Lorentz force

$$F_\alpha^E = -\frac{e}{m} \left(v_\mu F_\alpha^\mu - \frac{\omega_0}{m} F_\alpha^0 \right), \tag{4.59}$$

quantum force

$$F_\alpha^Q = \frac{1}{2m^2} \nabla_\alpha \left(\frac{\Box \sqrt{n}}{\sqrt{n}} \right), \tag{4.60}$$

gravitional "force"

$$F_\alpha^G = -2\nabla_\alpha \left(\frac{\omega_0^2}{4m^2 N^2} \right), \tag{4.61}$$

and conservative force

$$F_\alpha^n = -m \nabla_\alpha \mathcal{A}. \tag{4.62}$$

The emergence of these forces directly from generalized accelerations aligns with the principles of general relativity. Unlike classical mechanics, where forces are added externally, in this formalism the forces are derived from the equations of motion themselves, without having to be introduced arbitrarily. In the Newtonian limit, the equation (4.58) tends to

$$\partial_t \mathbf{v} + (\mathbf{v} \cdot \nabla) \mathbf{v} = -\nabla V_Q - \nabla \mathcal{A} + \frac{e}{m} (\mathbf{E} + \mathbf{v} \times \mathbf{B}). \tag{4.63}$$

The potential $V_Q = -(1/2m)\nabla^2 \sqrt{n}/\sqrt{n}$, which is associated with the quantum force,

refers precisely to the classical quantum potential discussed in the previous chapter, the gravitational "force" became null, since in the Newtonian limit the value of $N = 1$, the conservative force does not change because it depends on the arbitrary self-interacting potential and the Lorentz force takes its traditional form, with $(\mathbf{E}, \mathbf{B}) = (-\partial_t \mathbf{A} - \nabla \phi_E, \nabla \times \mathbf{B})$ being the electromagnetic field. As expected, we have arrived at an Euler-type equation for a fluid plus a quantum potential, as reported in [18].

Chapter 5

Stochastic Quantum Mechanics Applied to the Schwarzschild Metric

In the previous chapters of this thesis, we developed a theoretical framework to extend SQM to curved spaces. In this context, we proposed that the source of stochasticity lies in the intrinsic fluctuations of spacetime, whether due to background gravitational waves or other phenomena inherent to the fabric of spacetime. Through this approach, we showed how particle trajectories are affected by these fluctuations, transforming classical geodesics into stochastic trajectories. We concluded that the equation governing particles immersed in a curved and fluctuating spacetime is the Klein-Gordon equation.

In this chapter, we apply the SQM-CS formalism to the particular case of the Schwarzschild metric. Our objective is to find the stochastic trajectories of quantum particles and study how they are influenced by the Schwarzschild black hole. To this end, we begin by solving the Klein-Gordon equation for a massless scalar field in the Schwarzschild metric. We use these solutions to derive stochastic trajectories and

analyze the impact of parameters such as angular momentum, particle frequency, and initial conditions. Subsequently, we extend the analysis to the massive case, evaluating how the stochastic trajectories vary under these new conditions.

In this way, this chapter establishes a bridge between the theoretical formulation of SQM-CS and its application to the physical environment of a Schwarzschild black hole, providing a novel perspective on how spacetime fluctuations affect the dynamics of quantum particles in extreme gravitational scenarios.

5.1 Klein-Gordon Equation with a Massless Scalar Field in a Schwarzschild Background

The main objective in this section is to observe how scalar fields behave in a Schwarzschild black hole background. Specifically, we focus on a scalar field Φ that is massless, does not interact with itself, and is minimally coupled to the background geometry. The dynamics of this field are described by the Klein-Gordon equation

$$\Box\Phi(ct,\mathbf{r}) \equiv \nabla^\mu\nabla_\mu\Phi(ct,\mathbf{r}) = \sqrt{-g}\frac{\partial}{\partial x^\mu}\left[\sqrt{-g}g^{\mu\nu}\frac{\partial}{\partial x^\nu}\right]\Phi(ct,\mathbf{r}) = 0 \qquad (5.1)$$

where g is the determinant of the Schwarzschild metric[1]

$$ds^2 = \left(1 - \frac{r_s}{r}\right)d(ct)^2 + \left(1 - \frac{r_s}{r}\right)^{-1}dr^2 + r^2d\theta^2 + r^2\sin^2\theta d\phi^2, \qquad (5.2)$$

with the Schwarzschild radius defined as $r_s = 2MG/c^2$[2].

---

[1] The signature $(-,+,+,+)$ is taken.
[2] M, the mass of the black hole, G, the gravitational constant, and c, the velocity of light.

Let's assume that the energy associated with the scalar field configuration is quite small compared to the mass of the black hole (test field limit), so its gravitational contribution is minimal and negligible, making the entire geometric description dependent on the black hole's metric. Expanding equation (5.1), we find

$$- \left(1 - \frac{r_s}{r}\right) \frac{\partial^2 \Phi}{\partial t^2} \frac{1}{c^2} + \frac{1}{r^2} \left[\frac{\partial}{\partial r}\left[r^2 \left(1 - \frac{r_s}{r}\right)\frac{\partial \Phi}{\partial r}\right]\right] + \frac{1}{r^2 \sin\theta}\left[\frac{\theta}{\partial \theta}\left[\sin\theta \frac{\partial \Phi}{\partial \theta}\right]\right] + \frac{1}{r^2 \sin\theta}\frac{\partial^2 \Phi}{\partial \phi^2} = 0$$
$$(5.3)$$

Given that we have a spherically symmetric metric, it is natural to propose that the solution of (5.3) is a modal decomposition of the form

$$\Phi(ct, \mathbf{r}) = \frac{\Psi_l(ct, r)}{r} Y_l^m(\theta, \phi).$$
$$(5.4)$$

Replacing (5.4) in (5.3), we obtain

$$\frac{1}{c^2}\left(\frac{\partial^2 \Psi}{\partial t^2}\right) - \frac{r_s}{r^2}\left(1 - \frac{r_s}{r}\right)\left(\frac{\partial \Psi}{\partial r}\right) - \left(1 - \frac{r_s}{r}\right)^2 \left(\frac{\partial^2 \Psi}{\partial r^2}\right) + \overbrace{\left(1 - \frac{r_s}{r}\right)\left[\frac{r_s}{r^3} + \frac{l(l+1)}{r^2}\right]}^{V_l(r)} \Psi = 0.$$
$$(5.5)$$

with the potential $V_l(r)$ sometimes called "effective potential". The state mode ($l = 0$) and the first two excited states ($l = 1$ and $l = 2$) of the potential are plotted in Fig-(5.1). Let us note a few things about the potential: a) For each value of l, the potential $V_l(r)$ has a barrier shape, increasing up to a maximum and then decreasing as r increases. b) The potential is zero at the event horizon, $r = 2$ (for this illustrative case we take $G = c = 1$). c) For $l = 0$, the potential is lower compared to the values of $l = 1$ and $l = 2$, implying that modes with higher angular momentum feel a
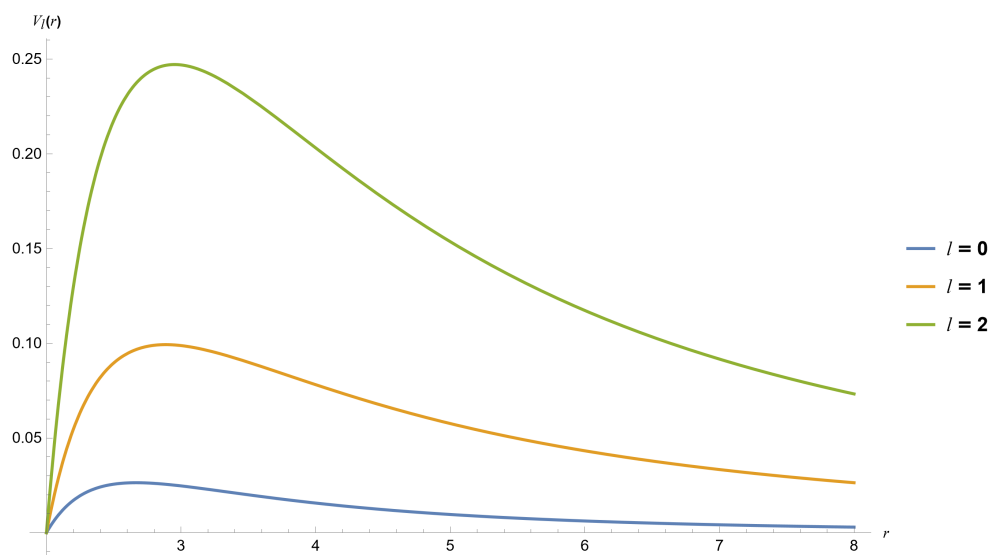
stronger barrier due to the curvature of spacetime.

Figure 5.1: Effective potential $V_l(r)$ as a function of r.

Let us extend the behavior of the potential $V(r)$ to the event horizon using the tortoise coordinates (2.5). We can visualize the potential $V(r^*)$ as seen in Fig-(5.2). Some of the main characteristics of $V(r^*)$ are: a) When $r = 2M$ then $r^* \to \infty$. Here, the behavior of the potential appears smoother (specifically, it decreases exponentially) and stays at zero. b) When $r = \infty$ then $r^* \to \infty$ (the potential decays as r^{-2}). c) The value of the potential increases (again) as l is larger. A detailed numerical analysis of the radial equation in tortoise coordinates is presented in [23]. The solution to this radial equation describes waves that are analyzed both in terms of scattering and in terms of quasi-normal modes, both phenomena affected by the effective potential acting as an effective barrier (see [24]). An exact solution in terms of the Confluent Heun function is found in [24] and it is precisely this solution (and its analysis) that we use in this work.
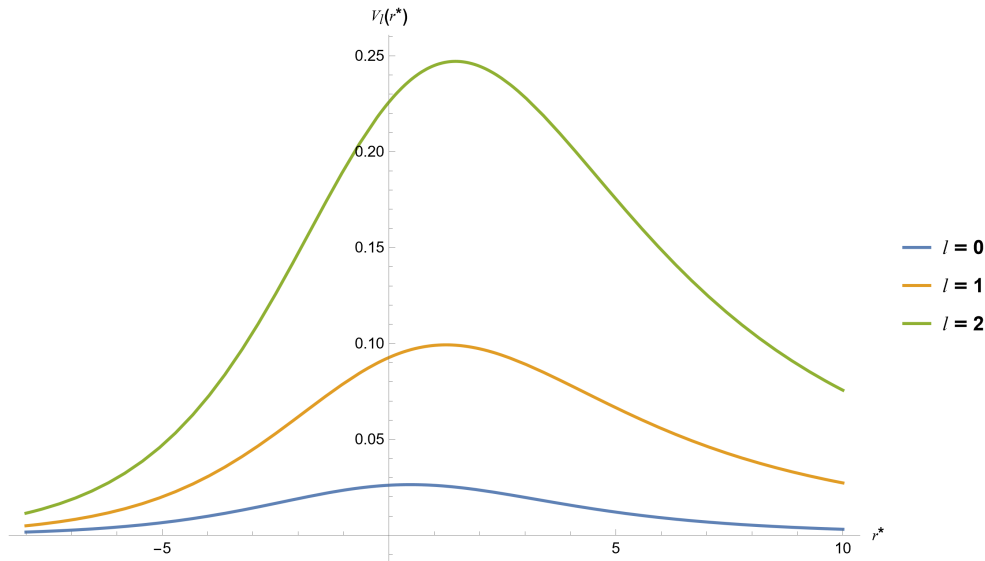
Figure 5.2: Effective potential $V_l(r^*)$ as a function of r^*.

The original Schwarzschild coordinate system (t, r) presents a problem as we approach the event horizon. As can be seen in equation (5.5), both $r = 0$ and $r = r_s$ (respectively the center of the Black-hole and the event horizon of the black hole), are supposedly singularities of the differential equation. However, $r = r_s$ is a removable singularity, which allows us to have information about what happens when crossing the event horizon.

With this in mind we use the ingoing Eddington-Finkelstein (E-F) coordinate to transform the equation (5.5). This procedure implies a coordinate transformation $(ct, r) \rightarrow (cv, u)$, with

$$cv = f(ct, r),\ u = g(ct, r). \tag{5.6}$$

Both angular variables, θ and ϕ remain invariant, ensuring that the coordinates are consistent with spherical symmetry. In equation (5.5) the partial derivatives with

respect to r (for example) mean that ct remains fixed (and vice versa). For our new coordinate system we will use the respective partial derivatives of u with cv fixed (and vice versa). The derivatives in the new coordinate system are given by:

$$\left.\frac{\partial}{\partial(ct)}\right|_{r=\text{cte}} = \dot{f}(ct,r)\frac{\partial}{\partial(cv)} + \dot{g}(ct,r)\frac{\partial}{\partial u}. \tag{5.7}$$

And the same for r:

$$\left.\frac{\partial}{\partial(r)}\right|_{t=\text{cte}} = f'(ct,r)\frac{\partial}{\partial(cv)} + g'(ct,r)\frac{\partial}{\partial u}. \tag{5.8}$$

Replacing the derivatives in (5.5), we see a differential equation of the form

$$
\begin{aligned}
&\left[\left(1-\frac{r_s}{r}\right)^2 f'^2 - \dot{f}^2\right] \frac{\partial^2\Psi(u,cv)}{\partial(cv)^2} \\
&+ \left[\left(1-\frac{r_s}{r}\right)^2 g'^2 - \dot{g}^2\right] \frac{\partial^2\Psi(u,cv)}{\partial u^2} \\
&+ \left[2\left(1-\frac{r_s}{r}\right)^2 f'g' - \dot{f}\dot{g}\right] \frac{\partial^2\Psi(u,cv)}{\partial u\partial(cv)} \\
&+ \left[\left(1-\frac{r_s}{r}\right)^2 f'' + \frac{r_s}{r^2}\left(1-\frac{r_s}{r}\right)f' - \ddot{f}\right] \frac{\partial\Psi(u,cv)}{\partial(cv)} \\
&+ \left[\left(1-\frac{r_s}{r}\right)^2 g'' + \frac{r_s}{r^2}\left(1-\frac{r_s}{r}\right)g' - \ddot{g}\right] \frac{\partial\Psi(u,cv)}{\partial u} \\
&- V_l(r)\Psi(u,cv) = 0,
\end{aligned}
\tag{5.9}
$$

where we have considered r to be a function of u and v ($r = r(u,v)$). We introduce the ingoing E-F coordinates by specifying the two functions ($f(r,t)$ and $g(r,t)$);

namely, in these coordinates we have

$$f = cv = ct + r + r_s \ln \left| \frac{r}{r_s} - 1 \right|, \tag{5.10}$$

$$g = u \equiv r. \tag{5.11}$$

Replacing these transformations, equation (5.9) reduces to

$$\left[\left(1 - \frac{r_s}{r} \right)^2 \frac{\partial^2}{\partial r^2} + 2 \left(1 - \frac{r_s}{r} \right) \frac{\partial^2}{\partial r \partial (cv)} + \frac{r_s}{r^2} \left(1 - \frac{r_s}{r} \right) \frac{\partial}{\partial r} - V_l(r) \right] \Psi(cv, r) = 0. \tag{5.12}$$

This differential equation can be separated into a purely radial equation using the ansatz

$$\Psi(cv, r) = e^{-i\omega cv} R_{\omega l}(r). \tag{5.13}$$

Inserting (5.13) into (5.12), we derive

$$\left[\frac{d^2}{dr^2} + \frac{r_s - 2i\omega r^2}{r(r - r_s)} \frac{d}{dr} - \left(\frac{l(l+1) + \frac{r_s}{r}}{r(r - r_s)} \right) \right] R_{\omega l}(r) = 0. \tag{5.14}$$

This radial differential equation has regular singularities at $r = 0$ (black hole singularity) and $r = r_s$ (event horizon). It also contains an irregular singularity at $r = \infty$ (you can notice this by taking $r \to 1/w$ and checking the behavior of $w = 0$). With these features in mind, this equation is part of a well-known type of differential equation (see Appendix (A)), the Heun confluent differential equation. To obtain the standard form of the Heun confluent equation we can make the transformation

given by

$$R_{\omega l}(r) = ry_{\omega l}(r), \tag{5.15}$$

which will give us the differential equation. For the rest of this discussion, we will adopt natural units and express all distances in terms of the Schwarzschild radius, $r_s = 2M$. With this choice, the event horizon is placed at $r = 1$.

$$\frac{d^2 y}{dr^2} + \left[\frac{1}{r} + \frac{1 - 2i\omega}{r - 1} - 2i\omega\right]\frac{dy}{dr} - \left[\frac{2i\omega + l(l+1)}{r - 1} - \frac{l(l+1)}{r}\right]y_{\omega l}(r) = 0. \tag{5.16}$$

Recall that the standard form of the Heun confluent equation (see equation (A.1)) is made up of 5 parameters, 2 regular singularities ($r = 1$ and $r = 2$) and one irregular one ($r = \infty$). The equation (5.16) has precisely the standard form and shares the 3 singularities. When comparing it with the equation (A.1), we identify the 5 parameters that characterize it as follows:

$$\gamma = 1,\ \delta = 1 - 2i\omega,\ \beta = 2i\omega,\ \alpha = 1 \text{ and } q = -l(l+1).$$

Two linearly independent solutions can be defined at the regular singularity $r = 1$, expressed using the confluent Heun function

$$R^I(r, 1) = ry_{\omega l}^I(r, 1) = r\text{HeunC}\left[-q + \alpha\beta, \alpha\beta, \delta, \gamma, \beta, 1 - r\right], \tag{5.17}$$

$$
\begin{aligned}
R^{II}(r, 1) = &ry_{\omega l}^{II}(r, 1) = r(r - 1)^{1-\delta}\text{HeunC}\left[-q + \alpha\beta + (\beta - \gamma)(1 - \delta),\right.\\
&\left.\alpha\beta + \beta(1 - \delta), 2 - \delta, \gamma, \beta, 1 - r\right].
\end{aligned} \tag{5.18}
$$

The two solutions are independent and show different behavior near the horizon.

The first solution remains regular and maintains a constant value at that location. Instead, the second solution makes an infinite number of turns on the unit circle in the complex plane and does not have a well-defined phase (see [24]).

5.2 Stochastic Trajectories with the Schwarzschild Metric

As mentioned in the introduction, the main goal of this thesis is to find the stochastic trajectories of quantum particles attracted by a Schwarzschild black hole and to analyze how these trajectories are affected by the strong associated gravitational field under the formalism of Stochastic Quantum Mechanics in curved spacetime. The previous section allowed us to determine the solution for a massless particle at the event horizon of a Schwarzschild black hole. Now, we can couple the incoming E-F metric (see equation (2.38)) to the systematic and stochastic velocity (see equations (4.26) and (4.27)) to solve the corresponding stochastic differential equations for the coordinates $x^\mu = (v, r, \theta, \phi)$ and thus obtain the particle trajectories. For massless particles, we propose $\mu = m = \omega_0$[3], where ω_0 is the frequency of the particle. From equation (4.8), we see that, in general, S is defined by[4]

$$S = \omega_0 x^0 - i\ln\left[\frac{\Phi}{\sqrt{\Phi\Phi^*}}\right].$$

(5.19)

---

[3]Using units, we would have $\mu = \dfrac{mc}{\hbar} = \dfrac{\omega_0}{c}$.

[4]Recall that in general the solution Φ is described by (4.6), where its amplitude Ψ is the Madelung transformation and the exponential part reflects a harmonic transformation, with x_0 being the evolution parameter. Therefore, the magnitudes or velocities proposed or calculated in the previous chapter, such as S, v^μ,π^μ, among others, will be written in terms of the evolution coordinate x^0, which for E-F is v.

The field equation that describes a quantum particle immersed in a curved and fluctuating spacetime is precisely the Klein-Gordon equation. The solution Φ of this equation serves as the function that determines the stochastic trajectory due to the influence of the surrounding. Therefore, we now consider the solution (5.4) as the function used to define these stochastic trajectories. Thus, by taking the incoming coordinates of E-F, we obtain S, which appears as follows

$$S = (\omega_0 - \omega)\, v - \frac{i}{2}\ln\left(\frac{\text{HeunC}}{\text{HeunC}^*}\right) + m\phi, \tag{5.20}$$

where we have abbreviated the Heun Confluent function to "HeunC" (the same for the complex conjugate "HeunC*" and m is associated with the spherical harmonics, $m = -l, -l+1, \ldots, l-1, l$.

The velocity of an individual particle (v^μ) is constructed from S (see (4.10) and note that in this case, we are not immersed in an electromagnetic field). We obtain

$$
\begin{aligned}
v^\mu = \Bigg[&-\frac{i}{2\omega_0}\partial_r\ln\left(\frac{\text{HeunC}}{\text{HeunC}^*}\right), \\
&\frac{(\omega_0-\omega)}{\omega_0} - 1 - \frac{i}{2\omega_0}\left(1-\frac{1}{r}\right)\partial_r\ln\left(\frac{\text{HeunC}}{\text{HeunC}^*}\right), 0, \frac{m}{r^2\sin^2\theta\,\omega_0}\Bigg].
\end{aligned}
\tag{5.21}
$$

Given v^μ, we construct π^μ with (4.26)

$$
\begin{aligned}
\pi^\mu = \frac{1}{2\omega_0}\Bigg[&-i\partial_r\ln\left(\frac{\text{HeunC}}{\text{HeunC}^*}\right), \\
&-i\left(1-\frac{1}{r}\right)\partial_r\ln\left(\frac{\text{HeunC}}{\text{HeunC}^*}\right) - 2\omega, 0, \frac{2m}{r^2\sin^2\theta}\Bigg].
\end{aligned}
\tag{5.22}
$$

The stochastic velocity (see (4.27)) is constructed with the particle density n; namely

$$n = \Phi\Phi^* = \text{HeunC HeunC}^* \left(Y_l^m(\theta, 0)\right)^2. \tag{5.23}$$

Making the respective calculations, we arrive at

$$
\begin{aligned}
u^\mu =& \frac{1}{2\omega_0} \left[\partial_r \left(\text{HeunC HeunC}^*\right),\right. \\
& \left.\left(1 - \frac{1}{r}\right) \partial_r \left(\text{HeunC HeunC}^*\right), \frac{1}{r^2}\partial_\theta \left(Y_l^m(\theta, 0)\right)^2, 0\right].
\end{aligned}
\tag{5.24}
$$

To find the stochastic trajectories, it is necessary to solve a differential equation of type (4.17). We have chosen to use a forward stochastic differential equation. The deterministic part U^μ, is defined as $U^\mu = \pi^\mu + u^\mu$ and its result is

$$
\begin{aligned}
U_+^\mu =& \frac{1}{2\omega_0} \left[-i\partial_r\ln\left(\frac{\text{HeunC}}{\text{HeunC}^*}\right) + \partial_r\left(\text{HeunC HeunC}^*\right),\right. \\
& \left.\left(1 - \frac{1}{r}\right)\left(i\partial_r\ln\left(\frac{\text{HeunC}}{\text{HeunC}^*}\right) - \partial_r\left(\text{HeunC HeunC}^*\right)\right) - 2\omega, \frac{1}{r^2}\partial_\theta\left(Y_l^m(\theta, 0)\right)^2, \frac{2m}{r^2\sin^2\theta}\right].
\end{aligned}
\tag{5.25}
$$

The Heun Confluent function is a complex function, and to solve the respective stochastic differential equation we use Mathematica in its 14.1 edition. In order for the program to process the calculation of the HeunC function, it is necessary to divide it into its real and imaginary parts

$$\text{HeunC} = \text{Re}[\text{HeunC}] + i\text{Im}[\text{HeunC}] = \text{R}[\text{H}] + i\text{I}[\text{H}], \tag{5.26}$$

$$\mathrm{HeunC}^* = \mathrm{Re}[\mathrm{HeunC}] - i\mathrm{Im}[\mathrm{HeunC}] = \mathrm{R}[\mathrm{H}] - i\mathrm{I}[\mathrm{H}]. \tag{5.27}$$

Replacing (5.26) and (5.27) in (5.25), we arrive at

$$U_+^\mu = \frac{1}{2\omega_0}\left[-2\left(\frac{\mathrm{R}[\mathrm{H}']\,(\mathrm{I}[\mathrm{H}] - \mathrm{R}[\mathrm{H}]) - \mathrm{I}[\mathrm{H}']\,(\mathrm{I}[\mathrm{H}'] + \mathrm{R}[\mathrm{H}])}{\mathrm{R}^2[\mathrm{H}] + \mathrm{I}^2[\mathrm{H}']}\right),\right.$$
$$\left.-2\left\{\left(1 - \frac{1}{r}\right)\left(\frac{\mathrm{R}[\mathrm{H}']\,(\mathrm{I}[\mathrm{H}] - \mathrm{R}[\mathrm{H}]) - \mathrm{I}[\mathrm{H}']\,(\mathrm{I}[\mathrm{H}'] + \mathrm{R}[\mathrm{H}])}{\mathrm{R}^2[\mathrm{H}] + \mathrm{I}^2[\mathrm{H}']}\right) - \omega\right\}, \frac{1}{r^2}\partial_\theta\,(Y_l^m(\theta,0))^2\,, \frac{2m}{r^2\sin^2\theta}\right].$$
$$\tag{5.28}$$

The associated diffusion coefficient in the system is $\sigma = 1/2m = 1/2\omega_0$[5]. As open source, the programming code can be consulted at ([25]). Each stochastic differential equation has an independent Wiener process (in particular, we will solve the coupled differential equations of $r(\tau)$ and $v(\tau)$). The stochastic process is defined using **ItoProcess**, which describes the evolution $r(\tau)$ and $v(\tau)$. **RandomFunction** is used to generate stochastic trajectories of the Itô process on a time interval τ and with a time step of 0.01. The two solutions are plotted with respect to the parameter τ and a parametric plot of $r(\tau)$ vs $v(\tau)$ is made.

Let us start by varying the radial initial condition $r(0)$. We will take two values close to the event horizon. The initial condition for the coordinate v is selected by setting $t = 0$ and knowing the radial initial condition (it must be remembered that the Schwarzschild radius is $r_s = 1$). In the Figs. (5.3, 5.4) we find the trajectories $r(\tau)$ and $v(\tau)$ with respect to the parameter τ by setting $l = 2, \omega_0 = \omega = 35$ and varying at $r(0) = 1.05r_s$ and $r(0) = 1.5r_s$ (7 trajectories for each solution). Physically, the

---

[5]If we use units, we would have $\sigma = \hbar/2m = c^2/2\omega_0$.

frequency $\omega_0 \approx 3 \times 10^{18}$Hz was used, which corresponds to X-rays[6]. The initial condition of $v(\tau)$ causes this trajectory to start at a different position than $r(\tau)$. It is also worth noticing that if the radial initial condition is placed closer to the black hole, the time trajectory will start at negative values (which is to be expected, since the shape of the transformation allows for this). The behavior of $v(\tau)$ with respect to τ varies much more than the radial trajectories do (this is much more noticeable in Fig (5.4)). The radial trajectory has a particular behavior. Both figures show that all radial trajectories will fall into the black hole (which is to be expected, since if one were to graph the geodesics π^μ, this is what one would obtain), but in different time intervals (parameter τ). For the initial condition $r(0) = 1.05r_s$ it was enough that τ varied between $[0, 0.8]$. For the other condition τ varied $[0, 1.17]$ because within this time the particles reach the origin $r = 0$. For the first case, being closer to the horizon, it will take less time to reach the singularity of the black hole (reason why the time is shorter, since if more time is iterated, the machine will reach the singularity and will not find a result at that point). For the second, it is the opposite, the further away, the longer it will take.

---

[6]The value of $\omega_0 = 35$ was proposed to emulate the value of σ with units.
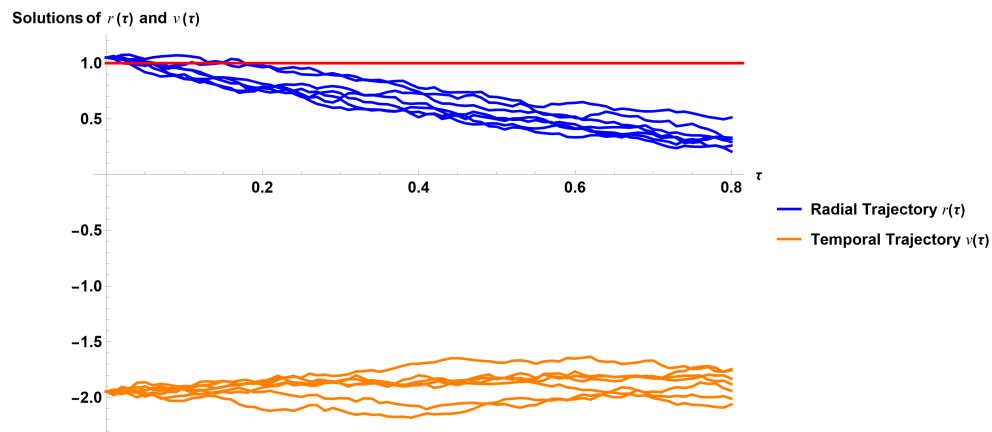
Solutions of $r(\tau)$ **and** $v(\tau)$

Figure 5.3: First variation $r(0) = 1.05 r_s$ and $v(0) = -1.94$. Trajectories $r(\tau)$ and $v(\tau)$. The red line shows the position of the event horizon.
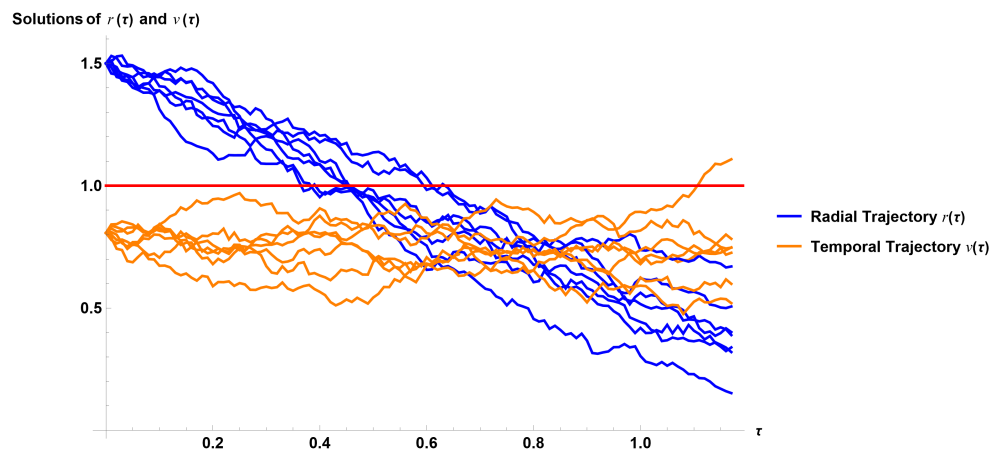
Solutions of $r(\tau)$ **and** $v(\tau)$

Figure 5.4: Second variation $r(0) = 1.5 r_s$ and $v(0) = 0.80$. Trajectories $r(\tau)$ and $v(\tau)$. The red line shows the position of the event horizon.

In the Fig. (5.4,5.5) we find the respective parametric graphs $r(\tau)$ Vs $v(\tau)$ of the two previous cases. Both graphs show the evolution of the particle in more detail. All trajectories are directed towards the singularity of the black hole (none escapes from the hole).
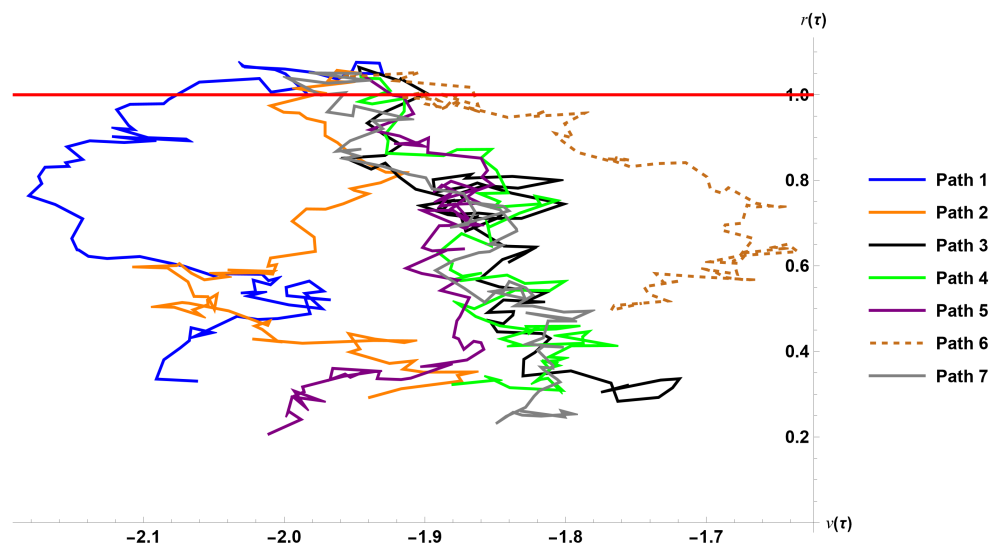
Figure 5.5: Firsts variation $r(0) = 1.05r_s$ and $v(0) = -1.94$. Trajectories $r(\tau)$ Vs $v(\tau)$. The red line shows the position of the event horizon.
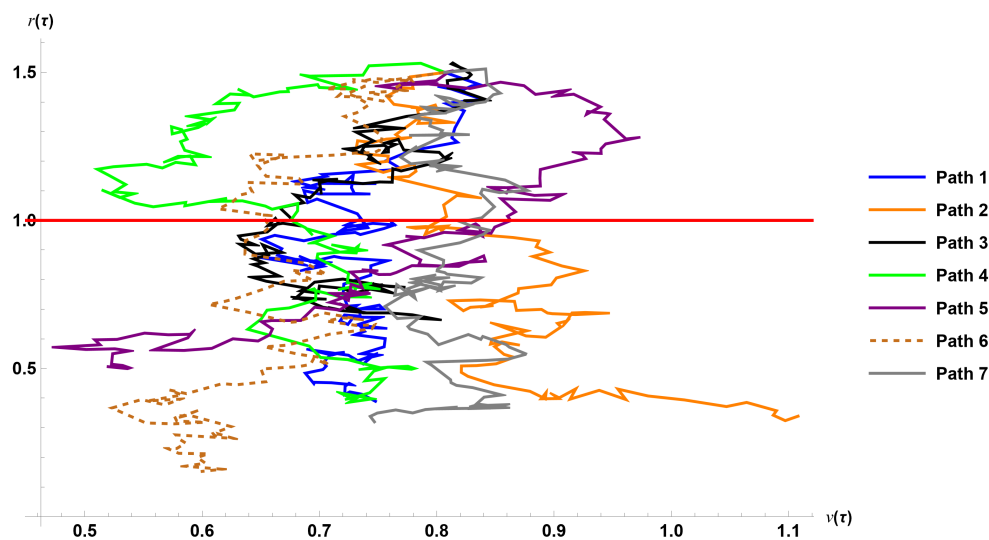

Figure 5.6: Second variation $r(0) = 1.5r_s$ and $v(0) = 0.80$. Trajectories $r(\tau)$ Vs $v(\tau)$. The red line shows the position of the event horizon.

Eddington Finkelstein coordinates allow us to obtain trajectories that, in advance,

can cross the event horizon. However, physically the parameter v does not give us information beyond describing incoming light trajectories (not the time evolution of stationary observers). For this reason, it is important to use the original coordinates (t, r, θ, ϕ), and analyze what an observer sees from afar; see Figs. (5.7, 5.8). The two graphs show similar things, the singularity (which is not a singularity but in these coordinates it is one) at the event horizon and the stochastic trajectories falling into the hole, which disappear every time they approach the event horizon. A solution is also drawn inside the event horizon, but it must be taken into account that it is not a valid solution in these coordinates, since, as is known, inside the black hole time is converted into space and vice versa. For a distant observer, what he will see is that the stochastic trajectories close to the event horizon will disappear and, likewise, an "infinite" time will be measured when touching the horizon (as expected).

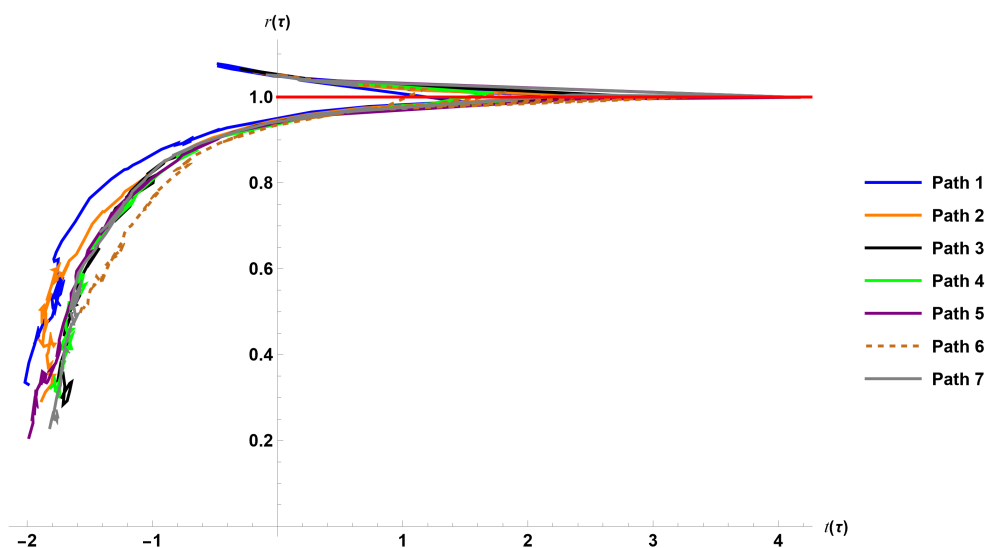Figure 5.7: Second variation $r(0) = 1.5r_s$ and $v(0) = 0.80$. Trajectories $r(\tau)$ Vs $v(\tau)$. The red line shows the position of the event horizon.
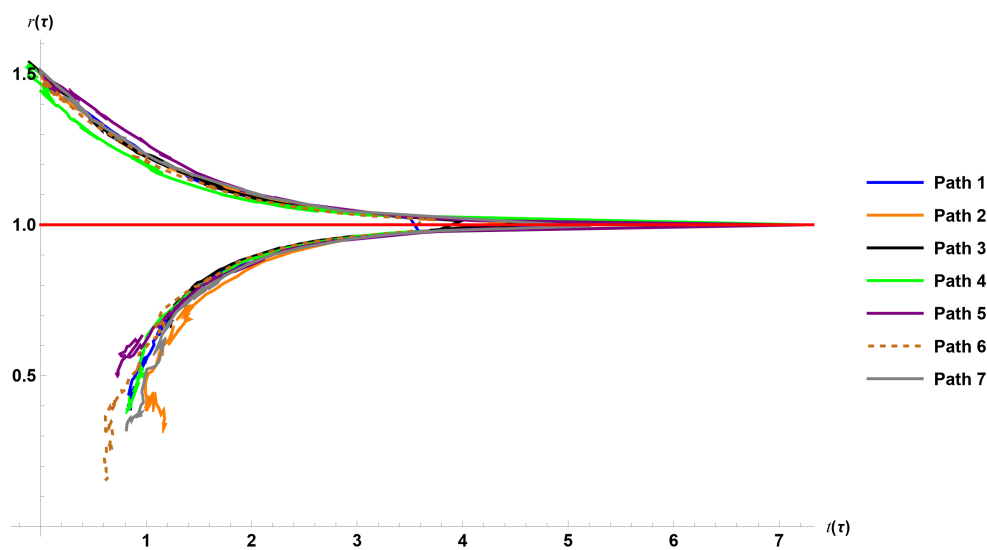
Figure 5.8: Second variation $r(0) = 1.5r_s$ and $v(0) = 0.80$. Trajectories $r(\tau)$ Vs $t(\tau)$. The red line shows the position of the event horizon.

The second parameter that can be varied is the angular momentum quantum number l. In Figs. (5.9, 5.10) the trajectories are shown as a function of τ for $l = 0$ and $l = 4$, with $\omega_0 = \omega = 35$ and $r(0) = 1.5r_s$. There are no abrupt changes in the behavior of the trajectories (both the radial trajectory and the time trajectory have the same behavior as in Fig. (5.4)). However, note that for $l = 0$, there are radial trajectories that take less time (time parameter τ) to reach the event horizon compared to trajectories with $l = 4$. Each computational iteration creates a new set of trajectories and this result was not always seen, but it is something that in theory should be expected, since for photons that do not have angular momentum $l = 0$, their trajectory is clearly radial (without angular affectation), and if l is larger, the trajectories are more complex. Another interesting result is that for $l = 0$ it is found that the particles stay longer inside the black hole before reaching the singularity

(the simulation was done in the interval $[0,1.4]$), while for the case where $l = 1$, they fall faster to the singularity (the simulation was done in the interval $[0,1.1]$).
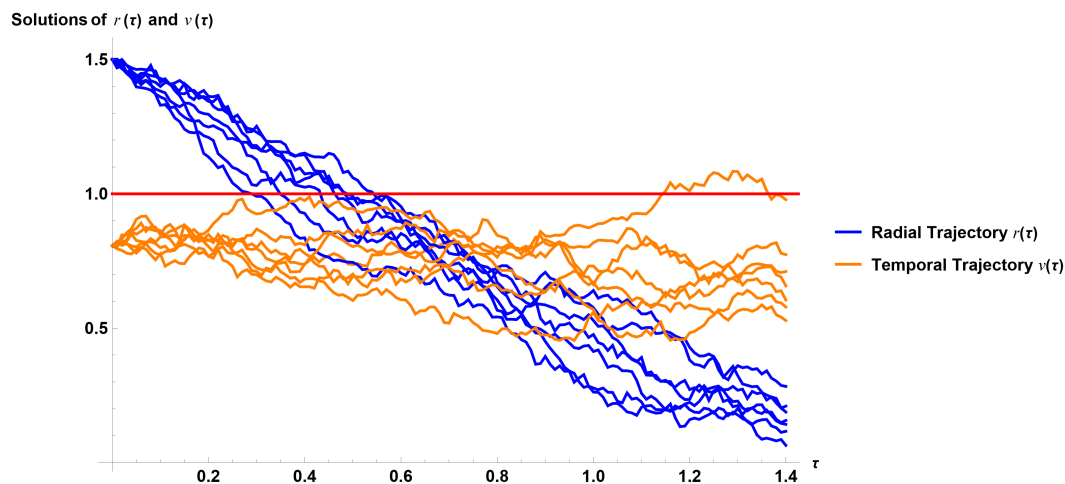

Figure 5.9: First variation $l = 0$. Trajectories $r(\tau)$ and $v(\tau)$ Vs τ. The red line shows the position of the event horizon.
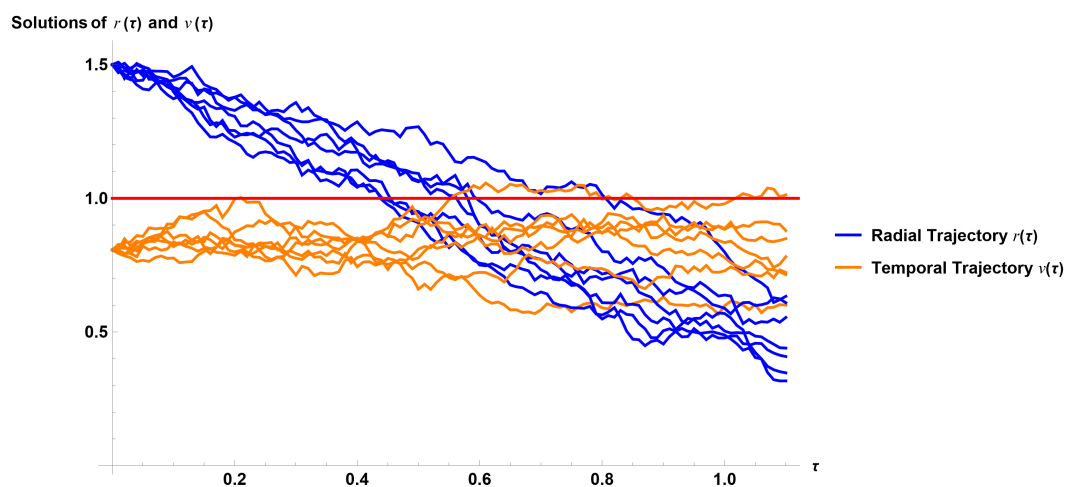

Figure 5.10: Second variation $l = 4$. Trajectories $r(\tau)$ and $v(\tau)$ Vs τ. The red line shows the position of the event horizon.

The last parameter we are going to vary is ω_0 (and in that order of ideas, also σ).

Physically we are using X-rays with a frequency around $\omega_0 \approx 3 \times 10^{18}$Hz (for the case of natural units, $\omega_0 = 35$). If we increase the frequency, the diffusion coefficient will decrease, finding increasingly deterministic trajectories, since the stochastic contribution will be small. In Fig. (5.11), with $\omega_0 = 1000$ (a value only for exemplification, since physically it would be a particle with too much energy) this behavior is quite clear, since the trajectories are smoother and their randomness is lower. If we decrease the frequency, the stochastic contribution will be greater, as we can see in Fig. (5.12). In this case $\omega_0 = 10$ (corresponds to less energetic X-rays) and it is noted that compared to the previous figures, there is greater randomness in the solutions. You might wonder why we don't take rays with lower energy, and the reason is simple: Solutions at lower frequencies imply more randomness and this in turn, more effort for the program. The stochastic differential equations to solve the system are complicated because the real and imaginary parts of the HeunC function must be calculated. As a result, the time with which the program iterates (τ), becomes shorter (a smaller interval) and for a comparison between a large and small value of ω_0 (with the same intervals of τ) we can only reach $\omega_0 = 10$.
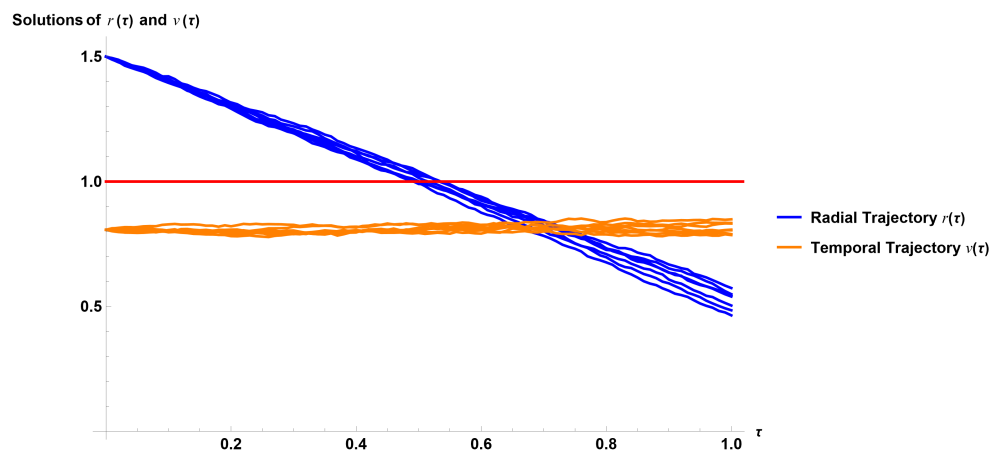
Solutions of $r(\tau)$ and $v(\tau)$

Figure 5.11: First variation $\omega_0 = 1000$. Trajectories $r(\tau)$ and $v(\tau)$ Vs τ. The red line shows the position of the event horizon.
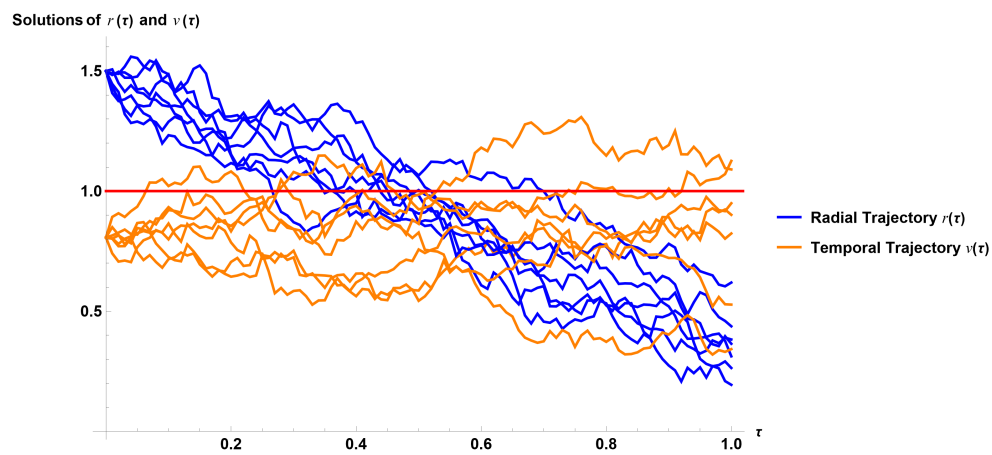
Solutions of $r(\tau)$ and $v(\tau)$

Figure 5.12: Second variation $\omega_0 = 10$. Trajectories $r(\tau)$ and $v(\tau)$ Vs τ. The red line shows the position of the event horizon.

For either of the last two cases (varying l or ω_0), the behavior of r Vs t remains the same, as in Figs. (5.7 and 5.8).

5.2.1 Case with mass $(m \neq 0)$

For the case with mass the system will have some peculiarities. The equation (5.12) will have an additional term corresponding to $\Box \Phi - \mu^2 \Phi = 0$ (where $\mu = m$[7]). Its temporal solution will be the same as in the previous case. Its radial solution, on the other hand, will now be of the form (falling again into a Confluent Heun-type equation, for more details see [26])

$$R^I(r,1) = r y^I_{\omega l}(r,1) = r e^{\left(i\omega + \sqrt{m^2 - \omega^2}\right)r} \text{HeunC}\left[-q + \alpha\beta, \alpha\beta, \delta, \gamma, \beta, 1 - r\right], \quad (5.29)$$

$$\begin{aligned}
R^{II}(r,1) =& r y^{II}_{\omega l}(r,1) \\
=& r e^{\left(i\omega + \sqrt{m^2 - \omega^2}\right)r}(r-1)^{1-\delta}\text{HeunC}\left[-q + \alpha\beta + (\beta - \gamma)(1 - \delta), \right. \quad (5.30) \\
& \left. \alpha\beta + \beta(1 - \delta), 2 - \delta, \gamma, \beta, 1 - r\right].
\end{aligned}$$

where the parameters of the confluent Heun equation of the standard form are given by

$$\gamma = 1, \ \delta = 1 - 2i\omega, \ \beta = -2\sqrt{m^2 - \omega^2}, \ \alpha = 1 - i\omega - \frac{m^2}{2\sqrt{m^2 - \omega^2}} + \frac{\omega^2}{\sqrt{m^2 - \omega^2}} \ \text{and}$$

$$q = -i\omega - l(l+1) - \sqrt{m^2 - \omega^2}.$$

The first solution is regular at the event horizon, while the second solution is not (for this reason we will use the first solution). A necessary condition at the horizon to have a system in which the incoming solution is regularly oscillatory and non-

---

[7]If we use units, we would have $\mu = mc/\hbar$

divergent and at infinity the solution is asymptotically flat, is that $m^2 < \omega^2$.

The solution (4.8) will change so that $\omega_0 = m$ (now, the frequency of the particle will be determined by the ω of the solution). Performing the same procedure as in the massless case, we find that the velocity π^μ is

$$
\pi^\mu = \frac{1}{2m} \left[2\omega - i\partial_r \ln\left(\frac{\text{HeunC}}{\text{HeunC}^*}\right), \omega\left(1 - \frac{1}{r}\right) - i\left(1 - \frac{1}{r}\right)\partial_r \ln\left(\frac{\text{HeunC}}{\text{HeunC}^*}\right) - \omega, 0, \frac{2m}{r^2 sin^2\theta} \right],
$$
$$(5.31)$$

$$
u^\mu = \frac{1}{2m} \left[\partial_r\left(\text{HeunC HeunC}^*\right) + 2\sqrt{m^2 - \omega^2}, \right.
$$
$$
\left. \left(1 - \frac{1}{r}\right)\left\{\partial_r\left(\text{HeunC HeunC}^*\right) + 2\sqrt{m^2 - \omega^2}\right\}, \frac{1}{r^2}\partial_\theta\ln\left(Y_l^m(\theta, 0)\right)^2, 0 \right],
$$
$$(5.32)$$

with $\sigma = 1/2m$[8]. If we add these two quantities, we obtain:

$$
U_+^\mu = \frac{1}{2m} \left[2\omega + i\partial_r\ln\left(\frac{\text{HeunC}}{\text{HeunC}^*}\right) + \partial_r\left(\text{HeunC HeunC}^*\right) + 2\sqrt{m^2 - \omega^2}, \right.
$$
$$
\left. -\frac{2\omega}{r} - i\left(1 - \frac{1}{r}\right)\partial_r\ln\left(\frac{\text{HeunC}}{\text{HeunC}^*}\right), \frac{1}{r^2}\partial_\theta\ln\left(Y_l^m(\theta, 0)\right)^2, \frac{2m}{r^2\sin^2\theta} \right].
$$
$$(5.33)$$

We require that $\omega^2 > m^2$, making the term $\sqrt{m^2 + \omega^2}$ imaginary. However, if this happens, the stochastic velocity (5.32) (and hence (5.33)) will be imaginary. For the present work it is beyond our main objectives to diagnose more precisely how to solve this stochastic velocity problem. Our conclusion, for the moment, is that for massive particles we will find no stochastic contribution to the velocity. The problem remains open for future investigations.

---

[8]If we use units, we would have $\sigma = c/2\mu = \hbar/2m$.

Chapter 6

Conclusions

In the present work, an approach to stochastic quantum mechanics in curved spaces has been developed, using as a theoretical basis the formalism followed by L. de la Peña and A. M. Cetto and Nelson [10, 11] and its extension to the context of curved spaces proposed by Escobar, Matos and Aquino [2]. The effects of the curvature of spacetime on quantum trajectories have been analyzed in detail, applying this stochastic formalism to the particular case of the Schwarzschild black hole.

By applying the 3+1 decomposition of spacetime and reformulating the Klein-Gordon equation in curved spacetimes, the deep connection between stochastic quantum dynamics and spacetime geometry has been demonstrated. This thesis shows that in curved spacetimes, stochastic fluctuations created by gravitational waves influence the trajectories of particles, creating stochastic trajectories.

In Chapter 5, we study configurations of massive and massless scalar fields in the vicinity of a Schwarzschild black hole using incoming Eddington-Finkelstein coordinates. The radial equation directly takes the form of the confluent Heun differential equation. This solution, represented as a Frobenius series expansion, is implemented

in the program Mathematica 14.1, which we will use as a reference for all simulations. The angular equation provides the spherical harmonics, and the temporal equation is solved using a classical exponential function.

The general solution is then used to find relevant quantities in the formulation of stochastic quantum mechanics in curved spacetimes. This allows us to determine the hydrodynamic and stochastic velocities of the system, and consequently, the stochastic trajectories of particles near the event horizon. Given the parameter $r(0)$, which varies the initial radial condition of the photon (in this case, X-rays), we observe that the farther the initial condition is from the event horizon, the longer it takes for the particle to fall into the black hole. Moreover, stochastic trajectories persist even when the initial radial condition is set farther away, leading us to conclude that these trajectories are not created by the black hole, but by the main hypothesis of the problem: the gravitational wave background (the fluctuation of spacetime); see Figs. (5.3, 5.4).

If we vary the angular momentum l of the particle (while keeping X-rays and distance $r(0)$ constant), we find that photons with no angular momentum fall into the black hole faster than those with angular momentum. This is expected because trajectories without angular momentum are purely radial, while those with angular momentum have an additional angular component, taking longer to fall; see Figs. (5.9, 5.10).

Finally, by varying the photon frequency, we observe that higher frequencies (higher energy) result in completely deterministic trajectories (as the diffusion coefficient decreases, reducing randomness). Conversely, lower energy photons (with

lower frequencies) exhibit more pronounced stochastic trajectories (increased diffusion coefficient and randomness); see Figs. (5.11, 5.12). Additionally, the computational process is more demanding for lower frequency photons due to longer iteration times. It is worth noting that, as with classical trajectories, distant observers will not see stochastic trajectories crossing the event horizon in the original Schwarzschild coordinates in any of the mentioned cases; see Figs. (5.7, 5.8)

The results suggest that stochastic quantum mechanics offers an alternative approach to exploring quantum effects in a gravitational context. While this thesis focuses on the Schwarzschild metric, the methods and findings are applicable to a variety of gravitational metrics and scenarios. This paves the way for future research in broader contexts, such as Kerr metrics or environments with more complex gravitational perturbations.

Bibliography

[1] Jonathan Oppenheim. A postquantum theory of classical gravity? *Phys. Rev. X*, 13:041040, Dec 2023.

[2] Eric S. Escobar-Aguilar, Tonatiuh Matos, and José I. Jimenez-Aquino. On the physics of the gravitational wave background, 2023.

[3] Agazie et al. The nanograv 15 yr data set: Evidence for a gravitational-wave background. *The Astrophysical Journal Letters*, 951(1):L8, June 2023.

[4] Daniel J. Reardon and Zic et al. Search for an isotropic gravitational-wave background with the parkes pulsar timing array. *The Astrophysical Journal Letters*, 951(1):L6, June 2023.

[5] Heng Xu and Chen et al. Searching for the nano-hertz stochastic gravitational wave background with the chinese pulsar timing array data release i. *Research in Astronomy and Astrophysics*, 23(7):075024, June 2023.

[6] EPTA Collaboration et al. The second data release from the european pulsar timing array - i. the dataset and timing analysis. *AA*, 678:A48, 2023.

[7] A. et al. Hees. Search for a variation of the fine structure constant around the supermassive black hole in our galactic center. *Phys. Rev. Lett.*, 124:081101, Feb 2020.

[8] A. M. Ghez, S. Salim, N. N. Weinberg, J. R. Lu, T. Do, J. K. Dunn, K. Matthews, M. R. Morris, S. Yelda, E. E. Becklin, T. Kremenek, M. Milosavljevic, and J. Naiman. Measuring Distance and Properties of the Milky Way's Central Supermassive Black Hole with Stellar Orbits. , 689(2):1044–1062, December 2008.

[9] Reinhard Genzel, Frank Eisenhauer, and Stefan Gillessen. The galactic center massive black hole and nuclear star cluster. *Rev. Mod. Phys.*, 82:3121–3195, Dec 2010.

[10] L. de la Peña, A.M. Cetto, and A.V. Hernández. *The Emerging Quantum: The Physics Behind Quantum Mechanics*. Springer International Publishing, 2014.

[11] Edward Nelson. Derivation of the schrödinger equation from newtonian mechanics. *Phys. Rev.*, 150:1079–1085, Oct 1966.

[12] S. Carroll, S.M. Carroll, and Addison-Wesley. *Spacetime and Geometry: An Introduction to General Relativity*. Addison Wesley, 2004.

[13] M. Alcubierre. *Introduction to 3+1 Numerical Relativity*. International Series of Monographs on Physics. OUP Oxford, 2008.

[14] Edward Nelson. *Dynamical theories of Brownian motion*. Mathematical Notes. Princeton University Press, first edition edition, 1967.

[15] Andrea Carosso. Simulating nelsonian quantum field theory. *Foundations of Physics*, 54(3), May 2024.

[16] Pierre-Henri Chavanis. Derivation of a generalized schrödinger equation from the theory of scale relativity, 2016.

[17] Erwin Madelung. Quantentheorie in hydrodynamischer form. *Zeitschrift für Physik*, 40:322–326, 1927.

[18] Tonatiuh Matos, Ana Avilez, Tula Bernal, and Pierre-Henri Chavanis. Energy balance of a Bose gas in a curved space-time. *Gen.Rel.Grav.*, 51(12):159, 2019.

[19] G. H. Derrick. Comments on Nonlinear Wave Equations as Models for Elementary Particles. *Journal of Mathematical Physics*, 5(9):1252–1254, 09 1964.

[20] Gerald Rosen. Existence of Particlelike Solutions to Nonlinear Field Theories. *Journal of Mathematical Physics*, 7(11):2066–2070, 11 1966.

[21] Pierre-Henri Chavanis. Derivation of a generalized schrödinger equation for dark matter halos from the theory of scale relativity. *Physics of the Dark Universe*, 22:80–95, 2018.

[22] T Zastawniak. A relativistic version of nelson's stochastic mechanics. *Europhysics Letters*, 13(1):13–17, sep 1990.

[23] Juan Barranco, Argelia Bernal, Juan Carlos Degollado, Alberto Diez-Tejedor, Miguel Megevand, Miguel Alcubierre, Dario Nunez, and Olivier Sarbach. Are black holes a serious threat to scalar field dark matter models? *Phys. Rev. D*, 84:083008, 2011.

[24] Dennis Philipp and Volker Perlick. On analytic solutions of wave equations in regular coordinate systems on schwarzschild background, 2015.

[25] Juan Sebastián Jerez Rodríguez. Quantum-mechanics-stochastics, 2024. Available at: https://github.com/JuanJerezPhysics/Quantum-Mechanics-Stochastics.

[26] Dennis Philipp and Volker Perlick. Schwarzschild radial perturbations in eddington–finkelstein and painlevé–gullstrand coordinates. *International Journal of Modern Physics D*, 24(09):1542006, 2015.

Appendix A

Confluent Heun Differential Equation

The Heun Confluent differential equation (a linear, homogeneous, ordinary second-order differential equation) has the form:

$$\left[\frac{d^2}{dz^2} + p_1(z)\frac{d}{dz} + p_0(z) \right] y(z) = 0 \tag{A.1}$$

where $p_i(z)$ are functions of rational coefficients and z is a point on the extended complex plane, also known as the Riemann sphere, which includes $z = \infty$.

When all singular points of a differential equation are regular, it is classified as a Fuchsian equation (otherwise, it is known as a confluent equation). The confluent Heun equation (CHE) belongs to the larger family of Heun equations and arises when two regular singularities of the general Heun equation (GHE) merge, forming an irregular singularity at $z = \infty$. Its standard form (see (A.1)), is accompanied by:

$$p_1(z) = \frac{\gamma}{z} + \frac{\delta}{z-1} - \beta, \tag{A.2}$$

$$p_0(z) = \left(\frac{\alpha\beta - q}{z - 1} + \frac{q}{z} \right). \tag{A.3}$$

The CHE has regular singularities at $z = 0, 1$ and an irregular singularity at $z = \infty$. Around the regular singularities we can build local Frobenius-type solutions. For the irregular singularity, we can build Thome-type solutions. For the singularity $z = 0$ we find

$$y^I(z; 0) = \sum_{k=0}^{\infty} a_k z^k, \tag{A.4}$$

$$y^{II}(z; 0) = \sum_{k=0}^{\infty} b_k z^{k+1-\gamma}. \tag{A.5}$$

For $z = 1$, the solution is

$$y^I(z; 1) = \sum_{k=0}^{\infty} c_k (z - 1)^k, \tag{A.6}$$

$$y^{II}(z; 1) = \sum_{k=0}^{\infty} d_k (z - 1)^{k+1-\delta}. \tag{A.7}$$

The coefficients of each solution can be found by replacing the solutions in the differential equation (A.1). We will find two linearly independent solutions, which we call I and II. To know in which singularity we are located, we take the notation $y^{I,II}(z; \cdot)$, with $(\cdot)$ indicating the singularity. These solutions are convergent within a circle in a complex plane, centered at the respective regular singularity with a radius that is the distance to the next neighboring singular point [24]. This standard form of the confluent Heun differential equation is not exactly the form that the Mathematica program handles as its standard form. However, the program itself rearranges its solution in such a way that, for the regular singularity $z = 0$, , the

standard confluent Heun function, with domain $|z| < 1$, is

$$y^I(z, 0) = \text{HeunC}[-1, -\alpha\beta, \gamma, \delta, -\beta, z], \tag{A.8}$$

$$y^{II}(z, 0) = z^{1-\gamma}\text{HeunC}[-1 + (1-\gamma)(-\beta-\delta), -\alpha\beta - \beta(1-\gamma), 2-\gamma, \delta, -\beta, z]. \tag{A.9}$$

and for the singularity $z = 1$, is

$$y^I(z, 1) = \text{HeunC}[-q + \alpha\beta, \alpha\beta, \delta, \gamma, \beta, 1-z], \tag{A.10}$$

$$y^{II}(z, 1) = (z-1)^{1-\delta}\text{HeunC}[-q+\alpha\beta+(\beta-\gamma)(1-\delta), \alpha\beta+\beta(1-\delta), 2-\delta, \gamma, \beta, 1-z]. \tag{A.11}$$

Solutions to the irregular singularity $(z = \infty)$ are created using the Thóme solution. Such solutions look like this:

$$y^I(z; \infty) = \sum_{k=0}^{\infty} \rho_k z^{-(k+\alpha)} \tag{A.12}$$

$$y^I(z; \infty) = e^{\beta z} \sum_{k=0}^{\infty} \sigma_k z^{-(k+\gamma+\delta-\alpha)}. \tag{A.13}$$

Again, the coefficients can be found by introducing the solutions of the differential equation (A.1). A way of relating all the solutions is given in [24]. For the purposes of the main objective of this thesis, what has been presented so far is sufficient.